

Comparison of benthic oxygen exchange measured by aquatic Eddy Covariance and Benthic Chambers in two contrasting coastal biotopes (Bay of Brest, France)

Polsenaere Pierre ^{1, 2, 3, *}, Deflandre Bruno ^{1, 2}, Thouzeau Gerard ⁴, Rigaud Sylvain ^{1, 2, 5}, Cox Tom ⁶, Amice Erwan ⁴, Bec Thierry Le ⁴, Bihannic Isabelle ⁷, Maire Olivier ^{1, 2}

¹ Université de Bordeaux, EPOC, UMR 5805, F-33400 Talence, France

² CNRS, EPOC, UMR 5805, F-33400 Talence, France

³ IFREMER, Laboratoire Environnement et Ressources des Pertuis Charentais (LER-PC), BP133, 17390, La Tremblade, France

⁴ LEMAR, UMR 6539 CNRS/UBO/Ifremer/IRD, Technopôle Brest-Iroise, Rue Dumont d'Urville, 29280 Plouzané, France

⁵ Université de Nîmes, EA 7352 CHROME, Laboratoire de Géochimie Isotopique Environnementale (GIS), 30035 NIMES Cedex 1, France

⁶ Royal Netherlands Institute for Sea Research (NIOZ), Ecosystem Studies Department, Korrिंगaweg 7, 4401 NT Yerseke, The Netherlands

⁷ LEMAR, UMR 6539 CNRS/UBO/Ifremer/IRD, Technopôle Brest-Iroise, Rue Dumont d'Urville, 29280 Plouzané, France

* Corresponding author : Pierre Polsenaere, email address : Pierre.Polsenaere@ifremer.fr

Abstract :

To the best of our knowledge, the understanding of benthic metabolism of coastal sedimentary areas is still limited due to the complexity of determining their true in situ dynamics over large spatial and temporal scales. Multidisciplinary methodological approaches are then necessary to increase our comprehension of factors controlling benthic processes and fluxes. An aquatic Eddy Covariance (EC) system and Benthic Chambers (BC) were simultaneously deployed during the winter of 2013 in the Bay of Brest within a Maerl bed and a bare mudflat to quantify and compare exchange at the sediment-water interface. Environmental abiotic parameters (i.e., light, temperature, salinity, current velocity and water depth) were additionally monitored to better understand the mechanisms driving benthic exchange. At both sites, EC measurements showed short-term variations (i.e. 15 min) in benthic fluxes according to environmental conditions. At the Maerl station, EC fluxes ranged from $-21.0 \text{ mmol m}^{-2} \text{ d}^{-1}$ to $71.3 \text{ mmol m}^{-2} \text{ d}^{-1}$ and averaged $22.0 \pm 32.7 \text{ mmol m}^{-2} \text{ d}^{-1}$ (mean SD), whilst at the bare muddy station, EC fluxes ranged from $-43.1 \text{ mmol m}^{-2} \text{ d}^{-1}$ to $12.1 \text{ mmol m}^{-2} \text{ d}^{-1}$ and averaged $-15.9 \pm 14.0 \text{ mmol m}^{-2} \text{ d}^{-1}$ (mean SD) during the total deployment. Eddy Covariance and Benthic Chambers measurements showed similar patterns of temporal flux changes at both sites. However, at the Maerl station, BC may have underestimated community respiration. This may be due to the relative large size of the EC footprint (compared to BC), which takes into account the mesoscale spatial heterogeneity (e.g. may have included contributions from bare sediment patches). Also, we hypothesize that the influence of bioturbation induced by large-sized mobile benthic fauna on sediment oxygen consumption was not fully captured by BC compared to EC. Overall, the results of the present study highlight the importance of taking into account specific

methodology limitations with respect to sediment spatial macro-heterogeneity and short-term variations of environmental parameters to accurately assess benthic exchange in the various benthic ecosystems of the coastal zone.

Highlights

► Benthic O₂ exchange was monitored in a temperate bay in winter. ► The aquatic Eddy Covariance and benthic chambers were deployed over two stations. ► Maerl beds and muddy sediments generally released and consumed O₂. ► Techniques showed similar patterns of temporal O₂ flux changes at both sites. ► Benthic chambers may have underestimated Maerl community respiration.

Keywords : benthic O₂ fluxes, aquatic Eddy Covariance, benthic chambers, Maerl bed, bare mudflat, Bay of Brest

73 1. Introduction

74
75 Coastal soft-bottom substrates represent active sites of biogeochemical cycling where
76 benthic communities of microbes and fauna deeply influence the fate (i.e. recycling, burial,
77 resuspension) of sedimented organic matter (Middelburg et al. 2004). Shallow marine
78 sediments can also support intense autotrophic production, thus controlling the metabolic
79 status (i.e. source or sink of carbon) of coastal marine systems (Jahnke et al. 2000). The
80 sediment oxygen consumption, assessed through the measurement of the total O₂ influx
81 across the sediment-water interface, provides an overall estimate of the total carbon turnover
82 rate (Glud 2008). In permeable sediments, physical processes, such as advective porewater
83 transport driven by current and wave actions strongly influence benthic O₂ exchange (Berg et
84 al. 2003, Reimers et al. 2012, Huettel et al. 2013, Berg et al. 2013). Conversely, in cohesive
85 sediments inhabited by diverse macrofaunal communities, benthic O₂ fluxes are
86 predominantly controlled by the biological mixing of the surficial sediment layer (i.e.
87 bioturbation), which encompasses both sediment reworking (i.e. particle transport) and bio-
88 irrigation (i.e. enhanced exchange of porewater and dissolved solutes across the sediment-
89 water interface) processes (Kristensen et al. 2012). However, the influence of bioturbation
90 activities on sedimentary biogeochemical processes is particularly difficult to accurately
91 assess at the scale of the whole habitat. Indeed, key processes (biological activities vs.
92 chemical redox reactions) typically occur at different spatial and temporal scales, which
93 cannot be simultaneously fully captured using classical methodologies. For instance, total
94 benthic O₂ exchange is typically quantified using incubation techniques either *in situ* or in
95 sediment cores incubated at the laboratory (McGlathery et al. 2001, Berg et al. 2003, Martin
96 et al. 2005, Huettel et al. 2007, Thouzeau et al. 2007, Khalil et al. 2013). Although
97 fundamental insights into the role of benthic fauna on biogeochemical processes have been
98 gained using both methodologies, benthic chambers (BC) have significant limitations. Firstly,
99 they most often consider small (or very small) sediment areas (i.e. a few tenths of m² in the
100 very best case) whereas large-sized bioturbating macrofauna often exhibits relatively low
101 densities and patchy distributions over much larger spatial scales. Moreover, the time required
102 to deploy BC or a sediment corer onto the seafloor, without disturbing the sediment-water
103 interface, does not allow for capturing the impact on solute exchanges of highly mobile (e.g.
104 flat fishes) or deep burrowing (e.g. thalassinid crustaceans) species, which can easily escape
105 from experimental enclosures before measurements are made. Yet, it is acknowledged that *in*
106 *situ* BC may significantly affect active transport processes and associated natural

107 hydrodynamic forcing at the sediment-water interface (Berg and Huettel 2008). Light
108 penetration can also be substantially reduced in BC compared to natural *in situ* conditions
109 (Tengberg et al. 2004).

110 The aquatic Eddy Covariance (EC) technique, developed by Berg et al. (2003), is expected to
111 solve such limitations. It allows the measurement of benthic O₂ exchange in a continuous
112 fashion and without being intrusive or disturbing the flow field over the sediment (Berg et
113 Huettel 2008). Furthermore, the sediment surface that contributes to the measured fluxes is
114 very large (10 to 100 m², Berg et al. 2007) in comparison to traditional incubation techniques.
115 Eddy Covariance measurements thus allow for taking into account the bioturbation activities
116 and the respiration of large mobile benthic fauna and overall to integrate the strong spatial
117 heterogeneity of complex coastal benthic systems. To date, this new alternative technique was
118 used to assess benthic metabolisms of various aquatic soft-bottom habitats, i.e. from lakes
119 (Brand et al. 2008, McGinnis et al. 2008, Lorrai et al. 2010), sandy-bottom river and sea
120 sediments (Berg et al. 2003, Chipman et al. 2012, Berg et al. 2013, Koopmans and Berg 2015,
121 Rovelli et al. 2017, Attard et al. 2019), vegetated and muddy lagoon sediments (Berg et al.
122 2003, Hume et al. 2011, Rheuban et al. 2014), vegetated and shallow sandy sea sediments
123 (Attard et al. 2019), sandy intertidal bays (Kuwaie et al. 2006, Berg et al. 2013), continental
124 shelf (Reimers et al. 2012) to deeper oceanic realms (Berg et al. 2009, Donis et al. 2016,
125 Attard et al. 2019). The use of the EC technique is particularly suitable over hard-bottom
126 substrates such as coral reefs (Long et al. 2013, Rovelli et al. 2015), Maerl beds (Attard et al.
127 2015), macroalgal and mussel reefs (Attard et al. 2019) and rocky embayments (Glud et al.
128 2010). In these latter rocky systems, incubation methods, which require a perfect sealing
129 between the chamber walls and the substratum, can be hardly deployed.

130 Maerl beds (i.e. unattached calcareous red algae communities developing at the surface of
131 shallow coastal sediments) are unique and complex habitats, somehow intermediate between
132 hard- and soft-bottom substrates. Accordingly, they host highly diverse biocenoses with
133 abundant autotrophic and heterotrophic organisms living within either the lattice of algae
134 thalli or the underlying sediment (Grall 2002, Barbera et al. 2003, Grall et al. 2006). Maerl
135 beds are considered among the most diversified and productive benthic ecosystems in the
136 world. However only few studies based on *in situ* incubation measurements, investigated their
137 biogeochemical functioning (Martin et al. 2005, 2007). Attard et al. (2015) have investigated
138 the biogeochemical functioning of a live Maerl bed community using an EC system, thus

139 showing that in the Scottish Loch Sween (1) O₂ exchange at the benthic interface are highly
140 dynamic, mainly driven by light availability and tidal flow, and (2) the benthic O₂
141 consumption exceeds O₂ production over a diel period. In the Bay of Brest, these complex
142 biogenic structures are particularly threatened by various human activities (mainly bivalve
143 dredging) (Hall-Spencer et al. 2003). To better predict the consequences of the accelerated
144 degradation of Maerl beds in the biogeochemical functioning of the whole Bay of Brest
145 ecosystem, similar studies investigating benthic organic matter remineralisation processes and
146 carbon cycling at large spatial scales are required.

147 In the present study, O₂ exchange was investigated at the sediment-water interface of two
148 contrasted biotopes, a Maerl bed and a bare muddy sediment, through simultaneous
149 deployments of an aquatic EC system and BC. The objectives were (1) to compare O₂ fluxes
150 measured at different spatial and temporal scales with EC and BC, (2) to assess short-term
151 dynamic in benthic O₂ exchange and to identify environmental controlling factors at the two
152 stations, and (3) to accurately quantify the benthic metabolism of the two studied biotopes in
153 the Bay of Brest.

154 2. Methods

156 2.1. Study site

158 The Bay of Brest is a semi-enclosed macrotidal marine ecosystem of about 180 km² located
159 in the West of France (Fig. 1). This coastal bay exchanges shelf waters with the Iroise Sea
160 through a narrow (2 km wide) and deep (40 m) strait. It receives moderate inputs of
161 freshwater from the Elorn and Aulne rivers that represent 80 % of the total freshwater inputs
162 (Chauvaud et al. 2000). The Bay is a shallow basin with more than 50 % of its surface
163 shallower than 5 meters (average depth 8 m). Tidal action induces short-term variability in
164 hydrological parameters and enhances mixing of the water masses (Chauvaud et al. 1998,
165 Thouzeau 2003). Maximal tidal range is 7.3 meters during spring tides. In the Bay of Brest,
166 Maerl beds cover more than one third of the benthic substrate (~ 60 km²) and develop from
167 the limit of spring low tides to a depth of 15 meters. They consist of cohesive muddy
168 sediments covered by a dense community of free-living coralline red algae, *Lithothamnion*
169 *corallioides* being the dominant species (Grall 2002). Though Maerl beds in the Bay of Brest
170 are of importance to sustainable fisheries, providing nursery grounds for commercial species

171 of fish and shellfish (i.e. scallops *Pecten maximus*, Hall-Spencer et al. 2003), the studied
172 Maerl bed was chosen because it had no anthropogenic disturbances during measurements.
173 Finally, the American slipper limpet *Crepidula fornicata* is also largely found in the Bay,
174 covering more than half of its benthic surface whilst seagrass meadows represent a much
175 smaller percentage of the area compared to Maerl beds in the Bay of Brest (Martin et al.
176 2007b, Ni Longphuir et al. 2007). *In situ* measurements were carried out during wintertime
177 of 2013, under anticyclonic conditions with cold and sunny weather and negligible surface
178 waves. Eddy Covariance and Benthic Chambers were simultaneously deployed within two
179 contrasted biotopes: a Maerl bed station located in the Northwest of the bay (48°21.916'N
180 04°26.006'W) and a bare muddy sediment station located in the South of the bay
181 (48°17.358'N 04°28.267'W) at five and ten meters deep, respectively (Fig. 1, Table 1).

2.2. Field measurements

2.2.1. Aquatic Eddy Covariance deployments

187 The different components of the EC system (Unisense A/S, version EC²) were mounted on a
188 custom-made stainless steel tripod frame specially designed to avoid, as far as possible,
189 hydrodynamic perturbation around sensors but able to sustain the natural hydrodynamic
190 forces in the Bay (Fig. 2A). Current velocity was measured by an acoustic Doppler
191 velocimeter (ADV with a fixed probe, Nortek vector) in a cylindrical measurement volume
192 (14 mm height and 14 mm in diameter) situated at 157 mm below the base of the three
193 transducers (Fig. 2B). The velocity was corrected against the speed of sound with water
194 temperature and salinity from the sampled station using the Vector software (1.34 version).
195 Oxygen concentration was measured by a Clark-type microelectrode from Unisense (< 25 µm
196 tip diameter) (Fig. 2B). All O₂ sensors used in this study had a 90 % response time below 0.3
197 seconds and a stirring sensitivity close to 2 %. The O₂ sensor was polarized at -0.8 volts for
198 24 hours before each deployment. An *in situ* eddy amplifier (ISA-Eddy, Unisense A/S) was
199 coupled to the microelectrode to amplify the total O₂ signal from the microelectrode and to
200 maximize signal-to-noise ratio, sensitivity and signal speed. The O₂ microelectrode was
201 positioned so that its tip was located as close as possible (< 1 cm) to the ADV measurement
202 volume (Fig. 2B). The signals generated by both the *in situ* eddy amplifier and the Nortek
203 vector were logged by the Unisense EC system controller unit (Fig. 2A). The EC controller

204 unit allowed deployment programming, storage (8 GB data capacity), power supply (internal
1 205 Li-ion batteries, approximately 34 hours at 25 °C of autonomy) and other unit interface
2
3 206 connections.

5 207 Water current velocity and O₂ concentration measurements were performed at 40 cm above
6
7 208 the substrate surface in continuous mode at 64 Hz. Additional sensors were set up on the EC
8
9 209 frame for measurement of environmental parameters. Oxygen concentrations were recorded
10
11 210 every ten seconds with an optode (4330F, Aanderaa) directly connected to the EC controller
12
13 211 unit. Another O₂ probe (SDOT300, NKE Instrumentation) equipped with a 3835 optode
14
15 212 (Aanderaa) was also used to monitor in parallel the O₂ in the bottom water and to calibrate the
16
17 213 microelectrode (see 2.3.1. section) (Fig. 2A). Both optodes were positioned at the same
18
19 214 distance above the substrate surface as the EC microelectrode tip. The optode signal was
20
21 215 checked by collecting triplicate samples of bottom water, in which the O₂ concentration was
22
23 216 analysed by Winkler titration. Temperature, salinity, pressure (water height) and
24
25 217 photosynthetically active radiation (PAR) were measured every two minutes by a STPS probe
26
27 218 (NKE Instrumentation) and a SPAR probe (NKE Instrumentation) equipped with a LI-COR
28
29 219 sensor, respectively (Fig. 2A).

30 220 At the two studied stations, the EC system was deployed from the boat but supervised by
31
32 221 IUEM SCUBA divers who (1) oriented the frame so that sensors were most of the time
33
34 222 downstream according to the main flow direction (negative x-current velocity), (2) ensured
35
36 223 that perturbation (i.e. frame position) and sediment re-suspension were the lowest possible,
37
38 224 and (3) removed potential obstructions such as rock, macro-algae, or maerl accumulations
39
40 225 close to the sensor axis that could lead to possible sensor damage or breaking.

41 226 EC deployments over Maerl bed and muddy sediment stations were carried out sequentially
42
43 227 during a two-day period in February 2013 and lasted from 11:30 to 17:30 (TU+1)
44
45 228 (2013/02/20) and from 11:30 to 18:30 (TU+1) (2013/02/21), respectively. Unfortunately, no
46
47 229 longer diurnal cycle deployments could be done at that time due to logistical reasons.

48 230

49 231 **2.2.2. Benthic chamber deployments**

50 232

51 233 Oxygen fluxes were simultaneously monitored using *in situ* large-sized benthic chambers
52
53 234 (see Thouzeau et al. 2007 for review). Three replicate enclosures made of 0.196 m²
54
55 235 cylindrical acrylic tubes (ca. 15 cm in height) were gently pushed into the substratum (Maerl
56
57 236 bed and bare muddy sediments) by SCUBA divers. The total enclosed volume was around 36
58
59 237 L slightly varying depending on the depth of insertion. A submersible pump connected to the
60
61
62
63
64
65

238 chamber and to waterproof batteries was adjusted to a fixed flow rate of 2 L min⁻¹ to
 239 homogenize the water inside the enclosures, corresponding roughly with the average
 240 hydrodynamics of the surrounding free-flowing water (Thouzeau et al. 2007). Transparent
 241 and dark chambers were used to determine net community production (NCP) and community
 242 respiration (CR), respectively. For each station, a set of three chambers (two transparent and
 243 one darkened) was simultaneously deployed for at least one hour. This procedure was
 244 repeated three times over the course of the daylight period from 11:00 to 15:00 (2013/02/20)
 245 and from 11:55 to 16:30 (2013/02/21) (TU+1) at the Maerl bed and bare muddy sediment
 246 stations, respectively. Each enclosure was opened for 30 minutes at least between each
 247 successive set of incubations to restore *in situ* conditions. Multiparameter probes (YSI
 248 6920v2) were used to continuously measure the oxygen concentrations, salinity, temperature
 249 and depth inside the chambers every minute. A LI-COR sensor (LI-192SA) was deployed
 250 near one of the clear BC to measure the light (PAR, 400-700 nm). Irradiance ($\mu\text{mol m}^{-2} \text{s}^{-1}$)
 251 was averaged every minute.

2.3. Data processing

2.3.1. EC data processing

257 The O₂ signal from the microelectrode was a millivolt reading (mv_{μ}) stored by time that
 258 linearly corresponds to the O₂ concentration. The O₂ microelectrode calibration was done
 259 from raw reading (mv_{μ}) converted to O₂ concentration ($[O_2]_{\mu}$, $\mu\text{mol L}^{-1}$) according to Eq (1).

$$[O_2]_{\mu} = [O_2]_{sdot} \times (mv_{\mu} - mv_0) / (mv_{sdot} \times mv_0) \quad (1)$$

261 where $[O_2]_{sdot}$ is the O₂ concentration ($\mu\text{mol L}^{-1}$) of the bottom water measured by the
 262 autonomous SDOT optode averaged over thirty minutes and corrected from water solubility,
 263 salinity and atmospheric pressure (Garcia and Gordon 1992, Hushida et al. 2008). The mv_{sdot}
 264 is the averaged O₂ signal in millivolt measured by the microelectrode over the same 30 min.
 265 averaging period, and mv_0 is the O₂ signal in millivolt that corresponded to the zero
 266 calibration obtained by immersing the microelectrode tip into an anoxic solution of sodium
 267 ascorbate and soda (2 g C₆H₈O₆ and 10 ml of 1 mol L⁻¹ NaOH completed to 100 ml with
 268 distilled water) before deployment.

269 Sediment-water O₂ fluxes, one for each 15 min. averaging time period or burst, were
 270 extracted from the high-resolution (64 Hz) raw data. The vertical turbulent eddy flux is
 271 defined as (2) (Berg et al. 2003).

$$\overline{FO_2} = \overline{u_z' C'} \quad (2)$$

where FO_2 is O_2 flux at the sediment-water interface measured by the aquatic EC technique, u_z' is the vertical turbulent fluctuating velocity and C' is the turbulent fluctuating O_2 concentration. The overbar represents a temporal average (i.e. 15 min. during this study), and primes denote the instantaneous turbulent fluctuations relative to their temporal average (e.g. $u_z' = u_z - \overline{u_z}$ and $C' = C - \overline{C}$, Reynolds 1895). Data were processed using the EC R-package (open source R software) developed by the NIOZ Institute (The Netherlands) (see Cathalot et al. 2015). Fluxes were then obtained from these raw EC data with a procedure involving several steps: (1) spike removal in vector and microelectrode O_2 data; (2) unit modifications and statistical operations on velocity and O_2 concentration; (3) coordinating rotation (two-axis rotation) on 3D velocity to align coordinate system with the stream lines of the 15 min. averages; (4) moving average filtering (window length of 100 seconds) to remove the mean (non-turbulent part of the covariance) from raw EC data; (5) determining and applying time shift correction for velocity and O_2 data using a cross-correlation procedure (shift window of ± 2 seconds); and (6) computing mean values, turbulent fluxes and characteristic parameters (i.e. noise analysis with standard deviation of first difference of v_z and O_2 , σ_{vz} and σ_{O_2} , respectively). In parallel, a (co)-spectral (variance preserving power spectra, average cumulative (co)-spectra ogive) analysis was carried out for each burst to quantify the distribution by frequency of the covariance of the raw measured signals. The sampling frequency (64 Hz), the short response time of the microelectrode (< 0.3 s) and the time averaging period (15 min.) allowed catching all contributing eddies (high and low frequency) to O_2 fluxes measured by EC. For more details on EC data processing, refer to Berg et al. (2003, 2009, 2013), Kuwae et al. (2006), McGinnis et al. (2008) and Lorrai et al. (2010). According to data quality control protocols, incorrect processed data have to be removed to obtain reliable O_2 fluxes. Several factors can lead to bias or errors, i.e. instrument malfunctioning, data processing artefacts, and natural *in situ* conditions not satisfying the assumptions of the EC methodology, i.e. non-stationary time series, convergence, divergence (Brand et al. 2008, Berg et al. 2009, Hume et al. 2011, Holtappels et al. 2013, Attard et al. 2014, Donis et al. 2015). Therefore, each 15 min. burst was carefully checked and we removed bursts that showed (1) ADV velocity data with a beam correlation threshold lower than 70 %, (2) standard deviations of first difference of v_z and O_2 , σ_{vz} and σ_{O_2} larger than 0.01 $m s^{-1}$ and 0.1 $\mu mol L^{-1}$, respectively, (3) deviations from the linearity of cumulative O_2 fluxes and (4) non steady-state conditions: the steady-state test was applied to pairs of specified signals, particularly to u_z and C in this study. Standard deviations and covariance of u_z and C

306 were computed on short time intervals of 1 min. and these values were compared to those
1 307 computed on the chosen time run of 15 min. following Foken and Wichura (1996). Only data
2 308 corresponding to a difference lower than 30 % (periods defined as steady-state conditions)
3 309 were retained. A clear linear trend within each burst indicates quasi-steady state conditions
4 310 with a constant O₂ flux and a statistically good representation of all eddy sizes that contribute
5 311 to the flux. In the end, 66 % and 54 % of the EC bursts were retained for further analysis in
6 312 the Maerl bed and the bare muddy sediments, respectively.

12 313 In order to estimate the surface area that contributes to EC O₂ flux (i.e. the footprint),
13 314 footprint calculations were done according to equations from Berg et al. (2007). The footprint
14 315 length (*l*), the upstream distance (*x*_{max}) and the footprint width (*w*) were computed from
15 316 measurement heights (*h*) and the roughness length (*z*₀) at each burst. The latter parameter was
16 317 obtained from the law of the wall from the measurement height (*h*), the mean current velocity
17 318 (\bar{u}), the von Karman's constant (*k* = 0.41) and the friction velocity (*u*_{*}) defined by Stull
18 319 (1988) (see Attard et al. 2015 for more details).

27 321 2.3.2. Benthic chamber data processing

29 322
30 323 Oxygen fluxes in the benthic chambers (BC) were calculated from the continuous O₂
31 324 concentrations during BC measurements in the overlying water as defined in Eq. 3.

$$34 325 FO_2 = (\Delta[O_2] \times V) / (A \times \Delta t) \quad (3)$$

35 326 where *FO*₂ is O₂ flux at the sediment-water interface (mmol m⁻² h⁻¹), Δ[O₂] is the variation in
36 327 the O₂ concentration during the incubation (mmol L⁻¹), *V* is the chamber volume (L), *A* is the
37 328 enclosed surface area (m²) and Δ*t* is the incubation time duration (hour). Net community
38 329 production (NCP) and community respiration (CR) were computed as mean O₂ fluxes
39 330 averaged over flux values measured during each sampling day by transparent and dark BC,
40 331 respectively.

49 333 2.3.3. Statistical tools

51 334
52 335 Post-processing (graphs and statistics) was performed using the GraphPad Prism version
53 336 6.00 software (La Jolla California USA, www.graphpad.com). The Shapiro-Wilk test was
54 337 used to test the normality of the data (with a *p* value below 0.05). The non-parametric test of
55 338 Mann-Whitney (with a *p* value below 0.01) was applied to distinguish significant differences
56 339 in benthic O₂ fluxes between stations and methodologies.

340 3. Results

1 341

3 342 3.1. Benthic O₂ exchange and associated environmental parameters at the Maerl station

5 343

7 344 Environmental parameters showed large variations during the 6.5 h deployment of the EC
8 system at the Maerl station (Fig. 3 and Table 1). Water height decreased from 6.3 m to 4.9 m.
9 345 High PAR values were recorded from 11:30 to 15:00 and reached values of up to 112 μmol
10 346 $\text{m}^{-2} \text{s}^{-1}$ around 14:00. PAR values suddenly dropped at 15:15 down to low values of ~ 2 μmol
11 347 $\text{m}^{-2} \text{s}^{-1}$ during the rest of deployment due to turbid riverine inputs into sub-surface water
12 348 bodies of the Bay with the ebbing tide (Fig. 3A). This sudden drop was not seen in any of the
13 349 other recorded environmental parameters. Water temperature and salinity at the sediment-
14 350 water interface increased steadily over the first two hours (from 8.9 to 9.7 °C and from 32.1 to
15 351 33.0, respectively), suggesting that warmer and saltier waters arrived with the flooding tide
16 352 (Fig. 3B). Water temperature and salinity then remained constant thereafter during the early
17 353 ebb tidal phase in the afternoon. Current velocities were in general low at the Maerl station
18 354 (from 1.0 to 7.4 cm s^{-1}) although short-term temporal variations were noticed. In particular, at
19 355 the beginning of the deployment the current first decreased from 5.1 to 1.0 cm s^{-1} over thirty
20 356 minutes and then increased to 6.9 cm s^{-1} one hour later (Fig. 3C). Oxygen concentrations
21 357 measured by the microelectrode and the SDOT optode (273 ± 3 $\mu\text{mol L}^{-1}$ on average) showed
22 358 weak variations during the deployment with values ranging from 269 to 279 $\mu\text{mol L}^{-1}$ (Fig.
23 359 3D and Table 1).

24 360 Large temporal changes in benthic O₂ fluxes were observed over the Maerl bed. EC fluxes
25 361 ranged from an uptake of -21.0 $\text{mmol m}^{-2} \text{d}^{-1}$ to a release of 71.3 $\text{mmol m}^{-2} \text{d}^{-1}$ and averaged
26 362 22.0 ± 32.7 $\text{mmol m}^{-2} \text{d}^{-1}$ during the total duration of the deployment (Fig. 3E, Table 1). Until
27 363 the observed sudden drop in PAR (i.e. 60 % of the time of the EC deployment), the Maerl
28 364 community showed a net O₂ production (47.2 ± 13.7 $\text{mmol m}^{-2} \text{d}^{-1}$ on average) associated with
29 365 the high PAR period (Fig. 3E). Benthic O₂ fluxes dropped suddenly in thirty minutes
30 366 concomitantly with the PAR decrease during the second half part of the deployment when a
31 367 net mean O₂ uptake of -13.9 ± 5.7 $\text{mmol m}^{-2} \text{d}^{-1}$ was measured (Fig. 3E). The footprint length,
32 368 the upstream distance to the location and the footprint width associated to EC fluxes over the
33 369 Maerl station were estimated to be between 63 and 257 m (mean of 171 ± 64 m), 2 and 10 m
34 370 (mean of 7 ± 3 m), and at 2.6 m, respectively (Table 1).

35 371 Transparent BC were deployed between 11:00 and 15:00 corresponding to the high PAR
36 372 period. They revealed high positive O₂ fluxes across the benthic interface. Oxygen fluxes
37 373

61
62
63
64
65

374 ranged from 64.8 to 105.7 mmol m⁻² d⁻¹ and averaged 87.4 ± 14.5 mmol m⁻² d⁻¹ (Table 1, Fig.
375 3E). In contrast, dark chamber incubations measured a community respiration (CR) ranged
376 between -44.0 and -33.3 mmol m⁻² d⁻¹ with a mean value of -38.6 ± 7.6 mmol m⁻² d⁻¹.

377

378 **3.2. Benthic Oxygen exchange and associated environmental parameters at the bare** 379 **muddy sediment station**

380

381 Large variations also occurred during the 7 h EC deployment at the bare muddy station (Fig.
382 4, Table 1). Water height was higher and ranged from 9.1 m to 11.0 m (Fig. 4A, Table 1).
383 PAR values were low during the whole duration of the deployment, decreasing from 17 μmol
384 m⁻² s⁻¹ at the beginning of the deployment (11:30) to 2 μmol m⁻² s⁻¹ afterwards (Fig. 4A).
385 Water temperature and salinity were steady with mean values of 9.6 ± 0.1 °C and 33.5 ± 0.1
386 (N=28), respectively (Table 1, Fig. 4B). Mean current velocity showed small variations from
387 2.4 to 5.8 cm s⁻¹ with a slight current decrease with the ebbing tide between 15:00 and 18:30
388 (Fig. 4C). Oxygen concentrations recorded by the EC microelectrode and the SDOT optode
389 showed weak temporal changes from 239 to 265 μmol L⁻¹ and averaged 248 ± 5 μmol L⁻¹
390 (Table 1, Fig. 4D).

391 Overall, sediment-water O₂ exchange measured by EC was negative and variable at the bare
392 muddy station, ranging from -43.1 to 12.1 mmol m⁻² d⁻¹, with a mean value of -15.9 ± 14.0
393 mmol m⁻² d⁻¹ (Table 1, Fig. 4E). A net O₂ uptake (-19.4 ± 11.3 mmol m⁻² d⁻¹ on average) was
394 measured during 88 % of the time. Large short-term variations in this O₂ uptake were
395 observed over short time scales (fifteen minutes at maximum) as for instance at the beginning
396 of the deployment with an O₂ uptake decrease from -28.0 to -6.7 mmol m⁻² d⁻¹ between 11:37
397 and 11:52 (Fig. 4E). O₂ flux shifts from negative to positive values also occurred (i.e. from -
398 43.1 to 12.1 between 14:52 and 15:22, Fig. 4E) although most of them were removed with our
399 data quality procedure (i.e. stationary test). The footprint length, the upstream distance to the
400 location and the footprint width associated to these fluxes at the mud station were comparable
401 to footprint characteristics computed at the Maerl station, and were estimated to be between
402 57 and 195 m (mean of 115 ± 35 m), 2 and 10 m (mean of 5 ± 2 m), and at 2.6 m, respectively
403 (Table 1).

404 An O₂ uptake (net negative NCP) of -9.1 ± 4.2 mmol m⁻² d⁻¹ on average (ranging from -14.6
405 to -2.4 mmol m⁻² d⁻¹, Table 1) was measured by clear BC incubations deployed from 11:55 to
406 16:30 under similar PAR values (2.1-7.1 μmol m⁻² s⁻¹) (Fig. 4D). Community Respiration

407 values measured by dark benthic chambers were between -27.0 and -7.6 $\text{mmol m}^{-2} \text{d}^{-1}$ with a
408 mean of -18.7 ± 10.0 $\text{mmol m}^{-2} \text{d}^{-1}$.

409 **3.3. Comparison of aquatic Eddy Covariance and Benthic Chamber techniques**

411
412 During the present study, benthic O_2 exchange was investigated in both biotopes using two
413 different and complementary approaches for the measurement of benthic O_2 fluxes (Fig. 5,
414 Table 1). At the Maerl station, significant differences were found between benthic O_2 fluxes
415 measured by BC and EC averaged over the same time period (EC_n) (87.4 ± 14.5 and $44.5 \pm$
416 11.0 $\text{mmol m}^{-2} \text{d}^{-1}$, respectively; Mann-Whitney test, $p = 0.0004$) (Fig. 5, Table 1). At the bare
417 muddy sediment station, no significant differences were noticed between BC (-9.1 ± 4.2
418 $\text{mmol m}^{-2} \text{d}^{-1}$) and EC fluxes averaged over the same time period (EC_n), with -16.5 ± 8.5
419 $\text{mmol m}^{-2} \text{d}^{-1}$ (Mann-Whitney test, $p = 0.1276$).

420 Eddy Covariance O_2 exchange measured over the Maerl station (EC_N , 22.0 ± 32.7 mmol m^{-2}
421 d^{-1}) was significantly different from those measured over the mud station (EC_N , -15.9 ± 14.0
422 $\text{mmol m}^{-2} \text{d}^{-1}$) (Mann-Whitney test, $p = 0.0015$) (Fig. 5, Table 1). Similarly significant
423 differences were observed between O_2 exchange measured with BC over Maerl and mud
424 stations (Mann-Whitney test, $p = 0.0022$) (Fig. 5, Table 1).

425 **4. Discussion**

426 **4.1. Aquatic Eddy Covariance versus Benthic Chamber O_2 flux measurements**

427 *Benthic flux technique comparison over complex, heterogeneous and non-cohesive Maerl* 428 *substrates*

429
430 Biogeochemical fluxes can show strong spatial and temporal changes over complex
431 substrates such as Maerl beds, characterized by a strong spatial heterogeneity and intense
432 advective porewater transport and bio-irrigation due to large macrobenthic organisms (Glud et
433 al. 2003, Rheuban and Berg 2013). In the present study, benthic O_2 fluxes measured by BC at
434 the Maerl bed station were consistently higher than those measured with the EC technique
435 (EC:BC ratio of 0.4-0.6; Figs. 3E and 5, Table 1).

436 Beyond potential hydrodynamic perturbations caused by BC deployments (Viollier et al.
437 2003), the larger sediment footprint covered by EC measurements may fundamentally

441 contribute to the difference between O₂ fluxes measured with the two methods. Indeed, at 40
1 442 cm above the Maerl bed, the footprint model gave an estimated area of ~ 350 m² (i.e. 171 m
2 443 long for ca. 2.6 m wide) compared to ~ 0.2 m² with BC (Table 1). The larger EC footprint
3 444 thus allows for a more accurate integration of the mesoscale spatial heterogeneity of
4 445 sedimentary biotopes (e.g. taking into account the contribution of bare sediment patches in O₂
5 446 flux). However, it should be noticed that the station was specifically chosen in the middle of
6 447 an extended Maerl bed covering several hectares to ensure that the footprint was consistently
7 448 smaller than the bed edges.

14 449 Also, it is well known that Maerl beds shelter large macrobenthic organisms including worms,
15 450 bivalves, crustaceans and echinoderms (Kamenos et al. 2004a, 2004b, Grall et al. 2006,
16 451 Attard et al. 2015). They also represent nursery grounds for numerous species of demersal
17 452 fish (Kamenos et al. 2004). The presence of large bio-irrigating animals enhances sediment
18 453 reworking and bioirrigation processes, which in turn stimulates the microbial respiration, and
19 454 leads to higher sediment O₂ uptakes. For instance, Yahel et al. (2008) estimated that silty
20 455 sediment resuspension induced by benthic fish could increase benthic O₂ demand up to 3.5-
21 456 fold. Due to patchy distributions of large benthic organisms, BC methodology tends to
22 457 underestimate the effects of bioturbation processes and CR. It could thus partly explain the
23 458 lower positive O₂ fluxes measured over the Maerl bed station by EC catching a more realistic
24 459 *in situ* CR. Attard et al. (2015) also highlighted, over Maerl beds in Loch Sween, large
25 460 variations between their BC replicates and endorsed the difficulty of the method to integrate
26 461 larger spatial scales and resolve an O₂ uptake representative of the whole benthic community.
27 462 In any case, our assumption (possible CR underestimation with BC) verified during daytime
28 463 but not during nighttime periods would deserve longer deployments to address the influence
29 464 of spatial heterogeneity on O₂ flux measurements along with methodological artifacts and
30 465 temporal resolutions.

466 467 ***Benthic flux technique comparison over bare cohesive soft sediment substrates***

468
51 469 Contrary to the non-cohesive Maerl bed site, an overall good agreement was found between
52 470 EC and BC O₂ flux measurements over the cohesive bare muddy sediment site. Indeed, no
53 471 significant differences in benthic O₂ fluxes were measured using simultaneously BC and EC
54 472 methodologies suggesting that in homogeneous biotopes such as bare muddy sediments, the
55 473 BC methodology allows for accurate benthic O₂ flux measurements (Fig. 5, Tables 1 and 2).
56 474 Berg et al. (2003) also documented a great similarity in benthic O₂ fluxes measured by EC
57
58
59
60
61
62
63
64
65

475 and BC elsewhere in temperate bare muddy sediments (Table 2). Our results also suggest a
1 476 good BC representation of *in situ* faunal activity (probably dominated by smaller animals)
2
3 477 over homogeneous soft bottom cohesive sediments characterized by lower mesoscale
4
5 478 heterogeneity. Additionally, the good correspondence between both techniques could reveal a
6
7 479 weaker influence of environmental parameters, such as light or tidal currents on O₂ fluxes at
8
9 480 the muddy station (Fig. 4, Table 1). Indeed, these parameters showed lower mean values and
10
11 481 ranges of variations during the deployment compared to the Maerl site. In particular, the very
12
13 482 low irradiance values did not allow recording NCP whatever the sampling technique and did
14
15 483 rather correspond to CR (Tables 1 and 2). To the contrary, even in relatively homogeneous
16
17 484 habitats, large benthic O₂ exchange differences could occur between the two techniques as
18
19 485 soon as sporadic short-term events such as storms happen during measurements. Camillini et
20
21 486 al. (in press) showed over a *Zostera marina* station in the Baltic Sea, the occurrence of
22
23 487 elevated flow speeds and associated sediment resuspension could induce a 5-fold increase in
24
25 488 the O₂ uptake rates measured by EC compared to BC due to reduced compound (FeSx)
26
27 489 reoxidation during resuspension.

28
29 490 Another reason of this good matching relies on the EC data quality procedure we adopted
30
31 491 during this study. One important assumption that must fulfill EC techniques is to measure
32
33 492 vertical turbulent fluxes during stationary conditions. To our knowledge, although numerous
34
35 493 studies have considered non-steady state conditions in their flux filtering protocol, it is the
36
37 494 first time that an aquatic EC study applies robust stationary tests coming from the atmospheric
38
39 495 EC technique to identify non-stationary conditions and remove it from the measured datasets
40
41 496 (see M&M section 2.3.1 and associated references). Despite a smaller EC burst number
42
43 497 retained, it results in robust and real EC flux variations that better match those measured with
44
45 498 BC. For instance, at the muddy sediment station between 16:22 and 16:52, non-stationary
46
47 499 conditions occurred with a mean velocity decreasing from 4.2 to 3 cm s⁻¹ that led to an O₂
48
49 500 flux shift from -34.9 to 6.5 mmol m⁻² d⁻¹ (Fig. 4). This latter artificial positive flux value was
50
51 501 identified and removed. Overall, the EC data quality procedure previously described allowed
52
53 502 catching real EC O₂ flux variations (-43.1 to 12.1 mmol m⁻² d⁻¹ instead of -48.4 to 18.6 mmol
54
55 503 m⁻² d⁻¹ without stationary tests) that better matched BC flux measurements (-14.6 to -2.4
56
57 504 mmol m⁻² d⁻¹, Table 1).

505

506

507

508

61
62
63
64
65

4.2. Short-term variations in benthic O₂ exchange and associated flux controls

Environmental control of benthic fluxes over non-cohesive Maerl substrates

In the coastal ocean, larger amounts of light generally reach the bottom floor due to shallow depths particularly, which allows in turn benthic primary production. Several studies have quantified this light influence on benthic primary production. For instance, Attard et al. (2014, 2015) showed that light was the main driver of benthic O₂ production at a coralline red algae site in a Southwest Greenland fjord and at a Maerl site located in the Loch Sween. Over the Maerl bed station of the Bay of Brest, the highest NCP values were reached during the periods exhibiting highest PAR values and short temporal variations in O₂ fluxes driven by light were observed. The sudden PAR drop, due to possible turbid riverine inputs with the ebbing tide, led to an 8-fold decrease in benthic O₂ exchange within 30 minutes (Fig. 3A). This relationship resulted in a significant positive correlation between EC O₂ flux and PAR values (Fig. 6A). Martin et al. (2005) precisely showed from P-E curve calculations that available irradiance was the major factor influencing primary production of Maerl beds in the Bay of Brest, explaining up to 94 % of benthic exchange. EC studies carried out by Attard et al. (2014, 2015) showed that little light levels were sufficient to drive a net autotrophic status response with compensation irradiance (I_c) values (derived from simple linear fit models) of 6 and 16 $\mu\text{mol m}^{-2} \text{s}^{-1}$, respectively. These I_c values are in good agreement with the value of 22.7 $\mu\text{mol m}^{-2} \text{s}^{-1}$ estimated in the present study but lower than the spring value calculated by Martin et al. (2005) of 107.5 $\mu\text{mol m}^{-2} \text{s}^{-1}$ in a nearby Maerl bed in the Bay of Brest. This high value, in opposition to normal responses of communities dominated by red algae typically low light adapted, could be attributed according to authors, to a major photosynthetic contribution of epiphytic macro- and microalgae to the total community production.

Differences observed between EC and BC O₂ exchange at this station (Fig. 5) suggest the occurrence of other environmental parameters than PAR as controlling factors. Particularly, local hydrodynamics is expected to significantly influence benthic O₂ fluxes inducing short-term variability (Holtappels et al. 2013). Attard et al. (2015) computed EC O₂ exchange versus flow velocity in darkness at the Maerl station in Loch Sween, with a seasonal trend in the slope of the regression (i.e. smaller slope in winter). In the Bay of Brest, we had no correlation between the current velocity and O₂ flux since current velocity range was much lower at this station compared to Loch Sween. However, tidally driven water height significantly influenced O₂ fluxes with mostly positive values measured as soon as water

543 height was higher than 5.6 meters (Fig. 6B). Indeed, at the end of the flooding tide at this
1 544 station, clearer waters with more available light would have allowed a higher photosynthetic
2 545 activity of Maerl beds. In contrast to this, during the next part of the deployment, the presence
3 546 of riverine turbid water bodies coming with the ebbing tide and more specifically current-
4 547 induced turbidity generated a strong decrease in bottom PAR and could have led to the
5 548 decrease observed in EC O₂ flux. Berg et al. (2013) discussed the sudden effect of light on O₂
6 549 production that is largely decoupled from current flow patterns, except in the case of current-
7 550 induced turbidity. These results show that the aquatic EC technique, through high-resolution
8 551 flux measurements, helps to resolve the strong dynamic of benthic O₂ exchange observed over
9 552 such coastal systems. Further and longer EC deployments along with water turbidity
10 553 measurements are however necessary and should allow decoupling the superimposition of
11 554 environmental forcing to better understand their influence on benthic O₂ fluxes.
12 555

556 *Environmental control of benthic fluxes over bare muddy sediments*

557
27 558 Large variations in benthic O₂ exchange were recorded at the bare muddy station (Fig. 4).
28
29 559 Light availability cannot explain these variations as suggested by PAR values below 10 μmol
30 560 $\text{m}^{-2} \text{s}^{-1}$ during most of the deployment time. This low light level at the sediment-water
31 561 interface was likely due to higher water height and higher turbidity values compared to the
32 562 Maerl station. Over shallower (4.2 ± 2.5 m) bare sediments in winter in the Bay of Brest, Ni
33 563 Longphuir et al. (2007) estimated from P-E curve calculations, minimum saturating
34 564 irradiance values (E_k) of $57.8 \pm 28.7 \mu\text{mol m}^{-2} \text{s}^{-1}$. The microphytobenthic production was
35 565 thus not light-limited at 4 m depth in the study of Ni Longphuir et al. (2007), in contrast to
36 566 our deeper (10.4 ± 0.5 m) muddy site (PAR: $6.9 \pm 3.7 \mu\text{mol m}^{-2} \text{s}^{-1}$). Interestingly, the present
37 567 study did not point out correlations between O₂ fluxes and hydrodynamic parameters. In the
38 568 Bay of Brest, current velocity variations at the muddy station were weak between consecutive
39 569 bursts retained after our quality EC data procedure. Nevertheless, a decrease in current
40 570 velocity of only 2 cm s^{-1} led to a decrease in O₂ uptake by at least a factor of two (e.g. from
41 571 $16:22$ to $17:07$, the velocity decreased from 4.2 to 2.4 cm s^{-1} while O₂ uptake decreased from -
42 572 34.9 to $-17.8 \text{ mmol m}^{-2} \text{ d}^{-1}$; Fig. 4). Transient flow velocities and water hydrodynamic more
43 573 generally, could then explain a significant part of the variability observed our EC fluxes
44 574 during the tidal cycle as furthermore highlighted by Holtappels et al. (2013) through
45 575 theoretical EC flux calculations and turbulence modeling applied to field data.
46 576

577 4.3. Benthic metabolism of the contrasted biotopes studied in the Bay of Brest

1 578

3 579 *Primary production and respiration of coralline algae communities*

5 580

7 581 Coralline algae-dominated communities, associated with abundant heterotrophic organisms
8
9 582 living in the sub-layers of cohesive muddy sediments, form a complex habitat largely
10
11 583 involved in nutrient and organic matter recycling (Barbera et al. 2003, Martin et al. 2007b). In
12
13 584 temperate regions, slow-growing algae such as Maerl beds can significantly contribute to the
14
15 585 benthic primary production (Roberts et al. 2002, Martin et al. 2005). We measured by EC and
16
17 586 BC techniques net community production (NCP) (Table 1) that are consistent with previously
18
19 587 published values and reveal a strong contribution of Maerl beds and associated autotrophic
20
21 588 organisms to the benthic primary production. Attard et al. (2015) observed under similar
22
23 589 environmental conditions, though lower PAR values were reported, a close net daytime
24
25 590 production on average over Maerl beds in the temperate Loch Sween (Table 2). Martin et al.
26
27 591 (2007b), in winter over a Maerl bed located in the southern basin of the Bay of Brest,
28
29 592 measured by BC under very similar light conditions, a similar average NCP value (Table 2).
30
31 593 These measurements highlight the potential low-light adaptation of Maerl communities in the
32
33 594 terrestrial-influenced turbid water masses at this location in the Bay of Brest, close to the
34
35 595 Elorn River. The study of Attard et al. (2015) resolved this low-light adaptation of temperate
36
37 596 Maerl beds, when measuring the highest mean rate of daytime net O₂ release in winter. The
38
39 597 low value of minimum saturating irradiance estimated by Ni Longphuir et al. (2007) in
40
41 598 winter in the Bay of Brest also suggested an adaptation of the microphytobenthic
42
43 599 communities associated with Maerl beds to the reduced light levels reaching the sediment-
44
45 600 water interface.

46 601 Despite their high productivity, coralline-dominated communities remain generally
47
48 602 heterotrophic with community respiration (CR) values for temperate systems in the range of
49
50 603 the benthic communities dominated by macroalgae, i.e. from -72 to -240 mmol m⁻² d⁻¹
51
52 604 (Middelburg et al. 2004). Indeed, these high-biodiversity communities host a number of
53
54 605 heterotrophic organisms (microbial, microfauna, larger grazers) and sustain intense organic
55
56 606 matter mineralization (Martin et al. 2005). In the southern part of the Bay of Brest, Martin et
57
58 607 al. (2005, 2007b) concluded from their seasonal surveys that maerl communities were
59
60 608 heterotrophic systems (Table 2). Despite substantial benthic primary production, Attard et al.
61
62 609 (2015) also concluded after 300 hours of EC and BC measurements that Maerl beds in Loch
63
64 610 Sween were net heterotrophic during each seasonal sampling campaign (Table 2). The present
65

611 EC measurements also suggested a near-balanced or heterotrophic status of Maerl beds in the
612 Bay of Brest, although longer deployments should be required to confirm this metabolic
613 status. Assuming 9.6 daylight hours (Meteo France data), daily O₂ fluxes estimated from
614 hourly BC flux values revealed a net autotrophic status of Maerl beds with a positive NCP of
615 $35.0 \pm 5.8 \text{ mmol m}^{-2} \text{ d}^{-1}$. Positive NCP values obtained by BC in the present study seemed to
616 be due to lower CR values compared to those measured by Martin et al. (2005; 2007b) in the
617 Bay using the same technique (Table 2).

618 *Benthic metabolism of bare muddy sediments*

619
620 Sediment O₂ uptakes through EC measurements (Table 1) were mainly noticed at the bare
621 muddy station as observed elsewhere in other EC studies (Table 2). Our EC and BC
622 measurements are in good agreement with CR values measured by Martin et al. (2007a) in
623 winter in the Bay of Brest; dark BC were deployed over a muddy station covered by low
624 densities of *Crepidula fornicata*. Ni Longphuir et al. (2007) also found very similar CR
625 values in winter, with the same BC technique, at a bare sediment site in the Brest Strait
626 without any *C. fornicata* or coralline algae (Table 2). Assuming 9.7 daylight hours (Meteo
627 France data) during the day of deployment, daily O₂ fluxes estimated from hourly BC flux
628 values revealed a slightly net heterotrophic status of bare muddy sediments in the Bay of
629 Brest with GPP and CR values of 3.9 ± 2.3 and $-7.6 \pm 4.0 \text{ mmol m}^{-2} \text{ d}^{-1}$, respectively (Table
630 2). The few positive O₂ flux values measured at our station suggest a certain O₂ production by
631 microphytobenthos communities, though limited by reduced light availability. The same
632 result was found in BC data, when comparing net O₂ fluxes between light and dark
633 incubations (Fig. 4). However, these microphytobenthic production values are far below those
634 estimated by Ni Longphuir et al. (2007) in winter over shallower bare sediments in the Bay
635 of Brest from biomass-irradiance relationships obtained in one specific site (GPP: 15.3 ± 6.4
636 $\text{mmol m}^{-2} \text{ d}^{-1}$).

637 638 **Conclusion: perspectives and implications for the global functioning of the Bay**

639
640 This study performed measurements of benthic O₂ exchange by aquatic EC and BC
641 techniques over contrasting coastal biotopes: a non-cohesive Maerl substrate vs. cohesive bare
642 muddy sediments in the Bay of Brest (France). Using both techniques, and based on our
643 specific winter measurements, opposed ecological functioning were found since Maerl bed

644 communities and muddy sediments generally released and consumed O₂, respectively. The
1 645 present study highlights that O₂ flux variations and their controlling factors can be captured
2 646 by the EC technique on comparable spatial and temporal scales. It shows the real potential of
3 647 the EC technique in benthic O₂ flux assessment under true *in situ* conditions over large spatial
4 648 and temporal scales. However, our knowledge of flux dynamics is still limited due to the
5 649 complexity of flux controlling factors and their interactions. Efforts involving
6 650 multidisciplinary methodological approaches (with simultaneous EC and BC deployments)
7 651 are clearly necessary to go further in our comprehension of factors controlling benthic O₂
8 652 exchange. Such approaches will allow understanding at a larger scale the ecological and
9 653 biogeochemical functioning of coastal sedimentary areas, which are well known to be systems
10 654 particularly complex with a high degree of heterogeneity (Stockdale et al. 2009).
11
12
13
14
15
16
17
18
19
20

21 656 Acknowledgements

22 657
23
24
25 658 The EDDYCO project (INSU EC2CO/DRIL program) provided financial support for this
26 659 study. The Région Aquitaine (FEBBA project) and the IZOFLUX project from the French
27 660 National Research Agency (white program) funded the EC system. The Région Aquitaine
28 661 (FEBBA project) and the Vrije Universiteit Brussel supported the two-year postdoctoral
29 662 fellowships awarded to P.P. The development of the new EC system, EC², was realized in
30 663 collaboration with *Unisense A/S* and the NIOZ-Yerseke. We would like to express our thanks
31 664 to the INSU team from L'Albert Lucas and Henry Bouillard and Christian Portier from
32 665 EPOC. This work has been carried out within the framework of the Cluster of Excellence
33 666 COTE. We thank the two reviewers and Editor-in-Chief Gunnar Lauenstein for their
34 667 constructive comments that improved the clarity and overall quality of the manuscript.
35
36
37
38
39
40
41
42
43
44

45 669 Bibliography

- 46 670
47 671
48 672 Aller, R. C. 2014. Sedimentary diagenesis, depositional environments and benthic fluxes. In:
49 673 Holland H.D. and Turekian K.K. (eds.), *Treatise on Geochemistry*, Second Edition, **8**: 293-
50 674 334. Oxford: Elsevier.
51 675
52 676 Aller, R. C., R. N. Glud, D. McGinnis and S. Rysgaard. 2014. Seasonal rates of benthic
53 677 primary production in a Greenland fjord measured by aquatic eddy correlation. *Limnol.*
54 678 *Oceanogr.* **59**: 1555-1569. doi: 10.4319/lo.2014.59.5.1555.
55 679
56
57
58
59
60
61
62
63
64
65

- 680 Attard, K. M., H. Stahl, N. A. Kamenos, G. Turner, H. L. Burdett and R. N. Glud. 2015.
1 681 Benthic oxygen exchange in a live coralline algal bed and an adjacent sandy habitat: an eddy
2 682 covariance study. *Limnol. Oceanogr.* **53**: 99-115. doi: 10.3354/meps11413.
- 3 683
4 684 Attard, K. M., I. F. Rodil, R. N. Glud, P. Berg, J. Norkko, and A. Norkko. 2019. Seasonal
5 685 ecosystem metabolism across shallow benthic habitats measured by aquatic Eddy Covariance.
6 686 *Limnol. Oceanogr.* **4**: 79-86. <https://doi.org/10.1002/lol2.10107>
- 7 687
8 688 Aubinet, M., A. Grelle, A. Ibrom, U. Rannik, J. Moncrieff, T. Foken, A. S. Kowalski, P. H.
9 689 Martin, P. Berbigier, C. H. Bernhofer, R. Clement, J. Elbers, A. Granier, T. Grunwald, K.
10 690 Morgenstern, K. Pilegaard, C. Rebmann, W. Snijders, R. Valentini, and T. Vesala. 2000.
11 691 Estimates of the annual net carbon and water exchange of European forests: the EUROFLUX
12 692 methodology. *Adv. Ecol. Res.* **30**: 113-175.
- 13 693
14 694 Baldocchi, D. D. 2003. Assessing the eddy covariance technique for evaluating carbon
15 695 dioxide exchange rates of ecosystems: past, present and future. *Glob. Change Biol.* **9**: 479-
16 696 492.
- 17 697
18 698 Barbera, C., C. Bordehore, J.A. Borg, M. Glémarec, J. Grall, J. M. Hall-Spencer, C. H. De La
19 699 Huz, E. Lanfranco, M. Lastra, P.G. Moore, J. Mora, M.E. Pita, A.A. Ramos-Esplá, M. Rizzo,
20 700 A. Sánchez-Mata, A. Seva, P.J. Schembri, and C. Valle. 2003. Conservation and management
21 701 of northeast Atlantic and Mediterranean maerl beds. *Aquatic Conserv. Mar. Freshw. Ecosyst.*
22 702 **13**: 65-76.
- 23 703
24 704 Berg, P., M. H. Long, M. Huettel, J. E. Rheuban, K. J. McGlathery, R. W. Howarth, K. H.
25 705 Foreman, A. E. Giblin, and R. Marino. 2013. Eddy correlation measurements of oxygen
26 706 fluxes in permeable sediments exposed to varying current flow and light. *Limnol. Oceanogr.*
27 707 **58**: DOI: 10.4319/lo.2013.58.4.1329, 1329-1343.
- 28 708
29 709 Berg, P., R. N. Glud, A. Hume, H. Stahl, K. Oguri, V. Meyer, and H. Kitazato. 2009. Eddy
30 710 correlation measurements of oxygen uptake in deep ocean sediments. *Limnol. Oceanogr.*
31 711 *Meth.* **7**: 576-584.
- 32 712
33 713 Berg, P., and M. Huettel. 2008. Monitoring the Seafloor Using the Non-invasive Eddy
34 714 Correlation Technique: Integrated Benthic Exchange Dynamics. *Oceanogr.* **21**: 164-167.
- 35 715
36 716 Berg, P., H. Røy, and P. L. Wiberg. 2007. Eddy correlation flux measurements - the sediment
37 717 surface area that contributes to the flux. *Limnol. Oceanogr.* **52**: 1672-1684.
- 38 718
39 719 Berg, P., H. Røy, F. Janssen, V. Meyer, B. B. Jørgensen, M. Huettel, and D. de Beer. 2003.
40 720 Oxygen uptake by aquatic sediments measured with a novel non-invasive eddy-correlation
41 721 technique. *Mar. Ecol. Prog. Ser.* **261**: 75-83.
- 42 722
43 723 Brand, A., D. F. McGinnis, B. Wehrli, and A. Wüest. 2008. Intermittent oxygen flux from the
44 724 interior into the bottom boundary of lakes as observed by eddy correlation. *Limnol. Oceanogr.*
45 725 **53**: 1997-2006.
- 46 726
47 727 Camillini, N., K. M. Attard, B. D. Eyre, and R. N. Glud. (in press). Resolving community
48 728 metabolism of eelgrass *Zostera marina* meadows by benthic flume-chambers and eddy
49 729 covariance in dynamic coastal environments. DOI: <https://doi.org/10.3354/meps13616>
- 50
51
52
53
54
55
56
57
58
59
60
61
62
63
64
65

- 730 Cathalot, C., D. Van Oevelen, T. J. S. Cox, T. Kutti, M. Lavaleye, G. Duineveld and F. J. R.
1 731 Meysman. 2015. Cold-water coral reefs and adjacent sponge grounds: hotspots of benthic
2 732 respiration and organic carbon cycling in the deep sea. *Front. Mar. Sci.* **2**: 37. doi:
3 733 10.3389/fmars.2015.00037
4 734
- 6 735 Chauvaud, L., F. Jean, O. Ragueneau, and G. Thouzeau. 2000. Long-term variation of the Bay
7 736 of Brest ecosystem: benthic–pelagic coupling revisited. *Mar. Ecol. Prog. Ser.* **200**: 35-48.
8 737
- 9 738 Chauvaud, L., G. Thouzeau, and Y. M. Paulet. 1998. Effects of environmental factors on the
10 739 daily growth rate of *Pecten maximus* juveniles in the Bay of Brest. *J. Exp. Mar. Biol. Ecol.*
11 740 **227**: 83-111.
12 741
- 14 742 Chipman, L., M. Huettel, P. Berg, V. Meyer, I. Klimant, R. N. Glud, and F. Wenzhoefer.
15 743 2012. Oxygen optodes as fast sensors for eddy correlation measurements in aquatic systems.
16 744 *Limnol. Oceanogr. Meth.* **10**: 304-316.
17 745
- 19 746 Crusius, J., P. Berg, D. J. Koopmans, and L. Erban. 2008. Eddy correlation measurements of
20 747 submarine groundwater discharge. *Mar. Chem.* **109**: 77-85.
21 748
- 23 749 Donis, D., D. F. McGinnis, M. Holtappels, J. Felden and F. Wenzhoefer. 2016. Assessing
24 750 benthic oxygen fluxes in oligotrophic deep sea sediments (HAUSGARTEN observatory),
25 751 *Deep Sea Res. Part I: Oceanogr. Res. Pap.* **11**: 1-10.
26 752
- 28 753 Donis, D., M. Holtappels, C. Noss, C. Cathalot, K. Hancke, P. Polsenaere, F. Wenzhoefer, A.
29 754 Lorke, F. Meysman, R. N. Glud and D. F. McGinnis. 2015. An Assessment of the Precision
30 755 and Confidence of Aquatic Eddy Correlation Measurements. *Jour. of Atm. and Ocea. Tec.* **32**:
31 756 642-655. 10.1175/JTECH-D-14-00089.1.
32 757
- 34 758 Foken, T. and B. Wichura. 1996. Tools for quality assessment of surface-based flux
35 759 measurements, *Agr. Forest Meteorol.* **78**: 83-105.
36
- 37 760 Garcia, H. E., and L. I. Gordon. 1992. Oxygen solubility in seawater: Better fitting equations.
38 761 *Limnol. Oceanogr.* **37**: 1307-1312.
39 762
- 41 763 Glud, R. N., P. Berg, A. Hume, P. Batty, M. E. Blicher, K. Lennert, and S. Rysgaard. 2010.
42 764 Benthic O₂ exchange across hard-bottom substrates quantified by eddy correlation in a sub-
43 765 Arctic fjord. *Mar. Ecol. Prog. Ser.* **417**: 1-12.
44 766
- 46 767 Glud, R. N. J. Woelfel, U. Karsten, M. Köhl, and S. Rysgaard. 2009. Benthic microalgae
47 768 production in the Arctic: applied methods and status of the current database. *Bot. Mar.* **52**:
48 769 559-571.
49 770
- 51 771 Glud, R. N. 2008. Oxygen dynamics of marine sediments. *Mar. Biol. Res.* **4**: 243-289.
52 772
- 53 773 Glud, R. N., J. K. Gundersen, H. Røy, and B. B. Jørgensen. 2003. Seasonal dynamics of
54 774 benthic O₂ uptake in a semi enclosed bay: importance of diffusion and fauna activity. *Limnol.*
55 775 *Oceanogr.* **48**: 1265-1276.
56 776
57
58
59
60
61
62
63
64
65

- 777 Grall, J., F. Le Loc'h, B. Guyonnet and P. Riera. 2006. Community structure and food web
1 778 based on stable isotopes ($\delta^{15}\text{N}$ and $\delta^{13}\text{C}$) analyses of a North Eastern Atlantic maerl bed. J.
2 779 Exp. Mar. Biol. Ecol. **338**: 1-15.
- 3 780 Grall, J. 2002. Biodiversité spécifique et fonctionnelle du maerl : réponses à la variabilité de
4 781 l'environnement côtier. PhD thesis, Université de Bretagne Occidentale, Brest.
- 5 782
- 6 783 Hall-Spencer, J. M., J. Grall, P. G. Moore, and R. J. A. Atkinson. 2003. Bivalve fishing and
7 784 maerl-bed conservation in France and the UK - retrospect and prospect. Aquat. Conserv. Mar.
8 785 Freshw. Ecosyst. **13**: 33-41.
- 9 786
- 10 787 Holtappels, M., R. N. Glud, D. Donis, B. Liu, A. Hume, F. Wenzhöfer, and M. M. M.
11 788 Kuypers. 2013. Effects of transient bottom water currents and oxygen concentrations on
12 789 benthic exchange rates as assessed by eddy correlation measurements. J. Geophys. Res. **118**:
13 790 1157-1169.
- 14 791
- 15 792 Huettel, M., P. Berg and J. E. Kostka. 2013. Benthic exchange and biogeochemical cycling in
16 793 permeable sediments. Ann Rev Mar Sci, **6**: 23–51. 10.1146/annurev-marine-051413-012706.
- 17 794
- 18 795 Huettel, M., P. Cook, F. Janssen, G. Lavik, and J. J. Middelburg. 2007. Transport and
19 796 degradation of a dinoflagellate bloom in permeable sublittoral sediment. Mar. Ecol. Prog. Ser.
20 797 **340**: 139-153.
- 21 798
- 22 799 Huettel, M., and G. Gust. 1992. Impact of bioturbation on interfacial solute exchange in
23 800 permeable sediments. Mar. Ecol. Progr. Ser. **89**: 253-267, doi:10.3354/meps089253
- 24 801
- 25 802 Hume, A. C., P. Berg, and K. J. McGlathery. 2011. Dissolved oxygen fluxes and ecosystem
26 803 metabolism in an eelgrass (*Zostera marina*) meadow measured with the eddy correlation
27 804 technique. Limnol. Oceanogr. **56**: 86-96.
- 28 805
- 29 806 Jahnke, R. A., J. R. Nelson, R. L. Marinelli, and J.E. Eckman. 2000. Benthic flux of biogenic
30 807 elements on the Southeastern US continental shelf: influence of pore water advective
31 808 transport and benthic microalgae. Cont. Shelf Res. **20**: 109-127.
- 32 809
- 33 810 Kamenos, N.A., P. G. Moore and J. M. Hall-Spencer. 2004a. Small-scale distribution of
34 811 juvenile gadoids in shallow inshore waters; what role does maerl play? ICES J. Mar. Sc. **61**:
35 812 422-429.
- 36 813
- 37 814 Kamenos, N. A., P. G. Moore and J. M. Hall-Spencer. 2004b. Attachment of the juvenile
38 815 queen scallop (*Aequipecten opercularis* (L.)) to maerl in mesocosm conditions; juvenile
39 816 habitat selection. J. Exp. Mar. Biol. Ecol. **306**: 139-155.
- 40 817
- 41 818 Koopmans, D. J., and P. Berg. 2015. Stream oxygen flux and metabolism determined with the
42 819 open water and aquatic eddy covariance techniques. Limnol. Oceanogr. **60**: 1344-1355.
43 820 doi:10.1002/lno.10103
- 44 821
- 45 822 Kristensen, E., G. Penha-Lopes, M. Delefosse, T. Valdemarsen, C. Quintana and G. Banta.
46 823 2012. What is bioturbation? The need for a precise definition for fauna in aquatic sciences.
47 824 Marine Ecology Progress Series, **446**: 285-302. Doi:10.3354/meps09506.
- 48 825
- 49
- 50
- 51
- 52
- 53
- 54
- 55
- 56
- 57
- 58
- 59
- 60
- 61
- 62
- 63
- 64
- 65

- 826 Kristensen, E. 2000. Organic matter diagenesis at the oxic/anoxic interface in coastal marine
1 827 sediments, with emphasis on the role of burrowing animals. *Hydrobiologia*. **426**: 1-24.
2 828
- 3 829 Kuwae, T., K. Kamio, T. Inoue, E. Miyoshi and Y. Uchiyama. 2006. Oxygen exchange flux
4 830 between sediment and water in an intertidal sandflat, measured *in situ* by the eddy-correlation
5 831 method. *Mar. Ecol. Prog. Ser.* **307**: 59-68.
6 832
- 7 833 Khalil, K., M. Raimonet, A.M. Laverman, C. Yan, F. Andrieux-Loyer, E. Viollier, B.
8 834 Deflandre, O. Ragueneau and C. Rabouille. 2013. Spatial and temporal variability of sediment
9 835 organic matter recycling in two temperate eutrophicated estuaries. *Aquatic Geochem.* **19**: 517-
10 836 542.
11 837
- 12 838 Long, M. H., P. Berg, D. de Beer and J. C. Zieman. 2013. *In situ* coral reef oxygen
13 839 metabolism: an eddy correlation study. *PLoS ONE*. **8**(3): e58581.
14 840 Doi:10.1371/journal.pone.0058581.
15 841
- 16 842 Lorrain, C., D. F. McGinnis, P. Berg, A. Brand, and A. Wüest. 2010. Application of oxygen
17 843 Eddy Correlation in aquatic systems. *J. Atmos. Ocean Tech.* **27**: 1533-1546.
18 844
- 19 845 Maire, O., J. N. Merchant, M. Bulling, L. R. Teal, A. Grémare, J. C. Duchène and M. Solan.
20 846 2010. Indirect effects of non-lethal predation on bivalve activity and sediment reworking. *J.*
21 847 *Exp. Mar. Bio. and Ecol.* **395**: 30-36.
22 848
- 23 849 Martin, S., G. Thouzeau, M. Richard, L. Chauvaud, F. Jean and J. Clavier. 2007a. Benthic
24 850 community respiration in areas impacted by the invasive mollusk, *Crepidula fornicata* L.
25 851 *Mar. Ecol. Prog. Ser.* **347**: 51-60.
26 852
- 27 853 Martin, S., J. Clavier, L. Chauvaud, and G. Thouzeau. 2007b. Community metabolism in
28 854 temperate maerl beds. I. Carbon and carbonate fluxes. *Mar. Ecol. Prog. Ser.* **335**: 19-29.
29 855
- 30 856 Martin, S., J. Clavier, J.-M. Guarini, L. Chauvaud, C. Hily, J. Grall, G. Thouzeau, F. Jean and
31 857 J. Richard. 2005. Comparison of *Zostera marina* and maerl community metabolism. *Aqua.*
32 858 *Bot.* **83**: 161-174.
33 859
- 34 860 McGinnis, D. F., S. Cherednichenko, S. Sommer, P. Berg, L. Rovelli, R. Schwarz, R. N.
35 861 Glud, and P. Linke. 2011. Simple, robust eddy correlation amplifier for aquatic dissolved
36 862 oxygen and hydrogen sulfide flux measurements. *Limnol. Oceanogr. Meth.* **9**: 340-347.
37 863
- 38 864 McGinnis, D. F., P. Berg, A. Brand, C. Lorrain, T. J. Edmonds, and A. Wuest. 2008.
39 865 Measurements of eddy correlation oxygen fluxes in shallow freshwaters: Towards routine
40 866 applications and analysis. *Geophys. Res. Lett.* **35**, L04403, doi:10.1029/2007GL032747
41 867
- 42 868 McGinnis, D. F., I. C. Anderson and A. C. Tyler. 2001. Magnitude and variability of benthic
43 869 and pelagic metabolism in a temperate coastal lagoon. *Mar. Ecol. Prog. Ser.* **216**: 1-15,
44 870 doi:10.3354/meps216001
45 871
- 46 872 McGlathery, K. J., P. Berg and R. Marino. 2001. Using porewater profiles to assess nutrient
47 873 availability in seagrass-vegetated carbonate sediments. *Biogeochem.* **56**: 239-263.
48 874
49
50
51
52
53
54
55
56
57
58
59
60
61
62
63
64
65

- 875 Middelburg, J. K., C. M. Duarte and J. P. Gattuso. 2004. Respiration in coastal benthic
1 876 communities. In: del Giorgio PA, Williams PJB (eds). Respiration in aquatic ecosystems.
2 877 Oxford University Press, Oxford, p 206-224.
3 878
- 4 879 Ni Longphuir, S. N., J. Clavier, J. Grall, L. Chauvaud, F. Le Loc'h, I. Le Berre, J. Flye-
6 880 Sainte-Marie, J. Richard and A. Leynaert. 2007. Primary production and spatial distribution
7 881 of subtidal microphytobenthos in a temperate coastal system, the Bay of Brest, France.
8 882 Estuarine, Coastal and Shelf Science. **74**: 367-380, ISSN 0272-7714,
9 883 <http://dx.doi.org/10.1016/j.ecss.2007.04.025>.
10 884
- 12 885 Norling, K., R. Rosenberg, S. Hulth, A. Grémare, and E. Bonsdorff. 2007. Importance of
13 886 functional biodiversity and species-specific traits of benthic fauna for ecosystem functions in
14 887 marine sediment. Mar. Ecol. Prog. Ser. **332**: 11-23.
15 888
- 17 889 Polsenaere, P., E. Lamaud, J.-M. Bonnefond, V. Lafon, P. Bretel, B. Delille, J. Deborde, D.
18 890 Loustau and G. Abril. 2012. Spatial and temporal CO₂ exchanges measured by Eddy
19 891 Covariance over a temperate intertidal flat and their relationships to net ecosystem
20 892 production. Biogeosciences **9**: 249-268.
21 893
- 23 894 Rovelli, L., K. M. Attard, A. Binley, C.M. Heppell, H. Stahl, M. Trimmer and R.N. Glud.
24 895 2017. Reach-scale river metabolism across contrasting sub-catchment geologies: Effect of
25 896 light and hydrology. Limnol. Oceanogr. **62**: S381-S399. doi:10.1002/lno.10619
26 897
- 28 898 Rovelli, L., K. M. Attard, L. D. Bryant, S. Flögel, H. Stahl, J. M. Roberts, P. Linke and R. N.
29 899 Glud. 2015. Benthic O₂ uptake of two cold-water coral communities estimated with the non-
30 900 invasive eddy correlation technique. Mar. Ecol. Prog. Ser. **525**: 97-104. doi:
31 901 10.3354/meps11211
32 902
- 34 903 Reimers, C. E., T. Özkan-Haller, P. Berg, A. Devol, K. Mccann-Grosvenor, and R. D.
35 904 Sanders. 2012. Benthic oxygen consumption rates during hypoxic conditions on the Oregon
36 905 continental shelf: Evaluation of the eddy correlation method. J. Geophys. Res. **117**: 1-18,
37 906 C02021, doi:10.1029/2011JC007564
38 907
- 40 908 Reimers, C. E., R.A. Jahnke, and L. Thomsen. 2001. *In situ* sampling in the benthic boundary
41 909 layer. In: Boudreau BP, Jørgensen BB (eds) The benthic boundary layer. Oxford University
42 910 Press, New York, p 245-268.
43 911
- 45 912 Reynolds, O. 1895. On the dynamical theory of incompressible viscous fluids and the
46 913 determination of the criterion. Phil. Trans. R. Soc. Lond. A Math. Phys. Sci. **186**: 123-164.
47 914
- 49 915 Rheuban, J. E., P. Berg, K. J. McGlathery 2014. Ecosystem metabolism along a colonization
50 916 gradient of eelgrass (*Zostera marina*) measured by eddy correlation. Limnol. Oceanogr. **59**,
51 917 doi: 10.4319/lo.2014.59.4.1376.
52 918
- 54 919 Rheuban, J. E., and P. Berg. 2013. The effects of spatial and temporal variability at the
55 920 sediment surface on aquatic eddy correlation flux measurements. Limnol. Oceanogr. Methods
56 921 **11**: 351-359.
57 922
- 58 923 Roberts, R. D., M. Kühl, R. N. Glud and S. Rysgaard. 2002. Primary production of crustose
59 924 coralline red algae in a high arctic fjord. J. Phycol. **38**: 273-283.
60
61
62
63
64
65

925

1 926 Stockdale, A., W. Davison and H. Zhang. 2009. Micro-scale biogeochemical heterogeneity in
2 927 sediments: A review of available technology and observed evidence. *Earth-Science Reviews*
3 928 **92**: 81-97.

4 929 Stull R. B. 1988. Mean Boundary Layer Characteristics. In: Stull R.B. (eds) *An Introduction*
5 930 *to Boundary Layer Meteorology*. Atmospheric Sciences Library, **13**: Springer, Dordrecht

6 931
7 932 Tengberg, A., H. Stahl, G. Gust, V. Muller, U. Arning, H. Andersson, and P. Hall. 2004.
8 933 Intercalibration of benthic flux chambers I. Accuracy of flux measurements and influence of
9 934 chamber hydrodynamics. *Prog. Oceanogr.* **60**: 1-28, doi:10.1016/j.pocean.2003.12.001

10 935
11 936 Thouzeau, G., J. Grall, J. Clavier, L. Chauvaud, F. Jean A. Leynaert S. Ni Longphuir E.
12 937 Amice D. Amouroux.2007. Spatial and temporal variability of benthic biogeochemical fluxes
13 938 associated with macrophytic and macrofaunal distributions in the Thau lagoon (France). *Est.*
14 939 *Coast Shelf Sci.* **72**: 432-447.

15 940
16 941 Thouzeau, G., 2003. Fonctionnement des écosystèmes marins côtiers : d'une approche
17 942 populationnelle à une approche écosystémique. Mémoire d'Habilitation à Diriger des
18 943 Recherches (HDR), spécialité Océanologie Biologique, Université de Bretagne Occidentale,
19 944 Brest.

20 945
21 946 Thouzeau, G., 1991. Experimental collection of postlarvae of *Pecten maximus* (L.) and other
22 947 benthic macrofaunal species in the Bay of Saint-Brieuc, France. II. Reproduction patterns and
23 948 postlarval growth of five mollusc species. *J. Exp. Mar. Biol. Ecol.* **148**: 181-200.

24 949
25 950 Uchida, H., T. Kawano, I. Kaneko, and M. Fukasawa. 2008. *In Situ* Calibration of Optode-
26 951 Based Oxygen Sensors. *J. Atmos. Oceanic Technol.* **25**: 2271-2281.

27 952
28 953 Viollier, E., C. Rabouille, S. E. Apitz, E. Breuer, G. Chaillou, K. Dedieu, Y. Furukawa, C.
29 954 Grenz, P. Hall, F. Janssen, J. L. Morford, J. C. Poggiale, S. Roberts, T. Shimmield, M.
30 955 Taillefert, A. Tengberg, F. Wenzhöfer, U. Witte. 2003. Benthic biogeochemistry: state of the
31 956 art technologies and guidelines for the future of *in situ* survey. *J. Exp. Mar. Biol. Ecol.* **285-**
32 957 **286**: 5-31, doi:10.1016/S0022-0981(02)00517-8

33 958
34 959 Yahel, G., R. Yahel, T. Katz, B. Lazar, B. Herut, and V. Tunnicliffe. 2008. Fish activity: a
35 960 major mechanism for sediment resuspension and organic matter remineralization in coastal
36 961 marine sediments. *Mar. Ecol. Progr. Ser.* **372**:195-209.

37 962
38 963 Zemmeling, H. J., H. A. Slagter, C. van Slooten, J. Snoek, B. Heusinkveld, J. Elbers, N. J.
39 964 Bink, W. Klaassen, C. J. M. Philippart, and H. J. W. de Baar. 2009. Primary production and
40 965 eddy correlation measurements of CO₂ exchange over an intertidal estuary. *Geophys. Res.*
41 966 *Lett.* **36**, L119606, doi:10.1029/2009GL039285

51 967

52 968

53 969

54 970

55 971

56 972

57 973

58 974

59

60

61

62

63

64

65

975

1 976

2 977

3 978

4 979

Fig. 1. Localization of the two study sites in the Bay of Brest (red square in the France map), Ma: Maerl beds (48°21.916'N 04°26.006'W), Mu: bare muddy station (48°17.358'N 04°28.267'W).

7 981

8 982

Fig. 2. Image of the aquatic EC system. (A) The EC system and associated sensors carried by the frame: (1) the EC system controller unit. (B) Main EC sensors; (2) acoustic doppler velocimeter ADV and (3) Oxygen (O₂) microelectrode (Clark type) with *in situ* eddy amplifier. The ADV transducer (the black ring represents the water current *x* direction). The other associated sensors are (4) O₂ optode directly connected to the EC system controller unit (front leg), (5) O₂ optode autonomously deployed, (6) STPS sensor for temperature, salinity and pressure measurements and (7, behind the left leg) SPAR sensor for photosynthetically active radiation PAR measurements.

9 983

10 984

11 985

12 986

13 987

14 988

15 989

16 990

Fig. 3. Aquatic Eddy Covariance O₂ fluxes and associated environmental parameters over the Maerl bed station (20/02/2013, from 11:30 to 17:30). Averaged EC Data from burst 1 (11:37:30) corresponds to EC raw data (at 64 Hz) averaged over 15 minutes between 11:30:00 and 11:45:00. (A) Photosynthetically active radiation (PAR, $\mu\text{mol m}^{-2} \text{s}^{-1}$) and water height (H, meters), (B) Water temperature (T, °C) and salinity, (C) Mean water current velocity (cm s^{-1}), (D) O₂ concentration ($\mu\text{mol L}^{-1}$) measured by the microelectrode and *SDOT* optode and (E) Sediment/water O₂ fluxes measured by EC (EC FO₂, $\text{mmol m}^{-2} \text{d}^{-1}$). Averaged FO₂ measured by BC have been added (BC FO₂, $\text{mmol m}^{-2} \text{d}^{-1}$). Positive and negative FO₂ values represent O₂ production (from Maerl beds to water) and O₂ uptake (by Maerl beds), respectively.

17 991

18 992

19 993

20 994

21 995

22 996

23 997

24 998

25 999

26 1000

Fig. 4. Aquatic Eddy Covariance O₂ fluxes and associated environmental parameters over the bare muddy station (21/02/2013, from 11:30 to 18:30). See Fig. 3 caption for variable details.

28 1001

29 1002

30 1003

Fig. 5. Aquatic Eddy Covariance and Benthic Chamber O₂ fluxes comparison over Maerl bed (A) and bare muddy sediment (B) stations. EC fluxes (\pm standard deviations) were averaged over each corresponding BC incubation hour to allow comparisons; number of EC values used for calculations were 0, 4 and 4 at Maerl bed and 2, 3 and 3 at bare muddy sediment stations, respectively.

31 1004

32 1005

33 1006

34 1007

35 1008

Fig. 6. Benthic O₂ fluxes measured by EC over the Maerl bed station plotted as a function of photosynthetically active radiation (PAR) and water height (H). (A) $\text{FO}_2 = 0.6 \pm 0.1 \text{PAR} - 13.2 \pm 6.5$ ($R^2 = 0.76^*$, $p < 0.0001$, $n = 17$). (B) $\text{FO}_2 = 54.1 \pm 8.1 \text{H} - 291.4 \pm 47.4$ ($R^2 = 0.75^*$, $p < 0.0001$, $n = 17$).

37 1009

38 1010

39 1011

40 1012

41 1013

42 1014

43 1015

44 1016

45 1017

46 1018

47 1019

48 1020

49 1021

50 1022

51 1023

52 1024

53 1025

54 1026

55 1027

56 1028

57 1029

58 1030

59 1031

60 1032

61 1033

62 1034

63 1035

64 1036

65 1037

1029
11030
21031
31032
41033
51034
61035
71036

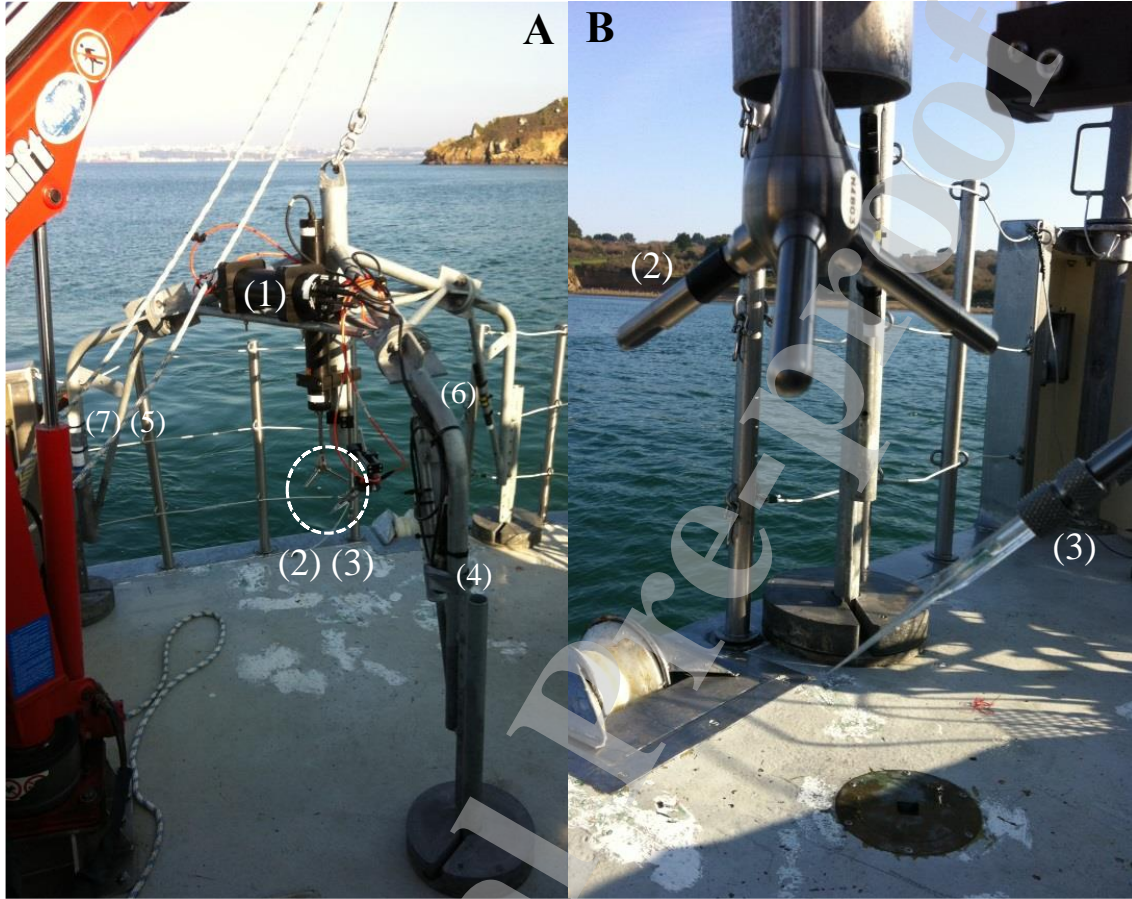
Fig. 1



9
10
11
12
13
14
15
16
17
18
19
20
21
22
23
24
25
26
27
28
29
30
31
32
33
34
35
36
37 1037
38 1038
39 1039
40 1040
41 1041
42 1042
43 1043
44 1044
45 1045
46 1046
47 1047
48 1047
49 1048
50 1049
51 1050
52 1051
53 1052
54 1053
55 1053
56 1054
57 1055
58 1056
59 1057
60 1058
61
62
63
64
65

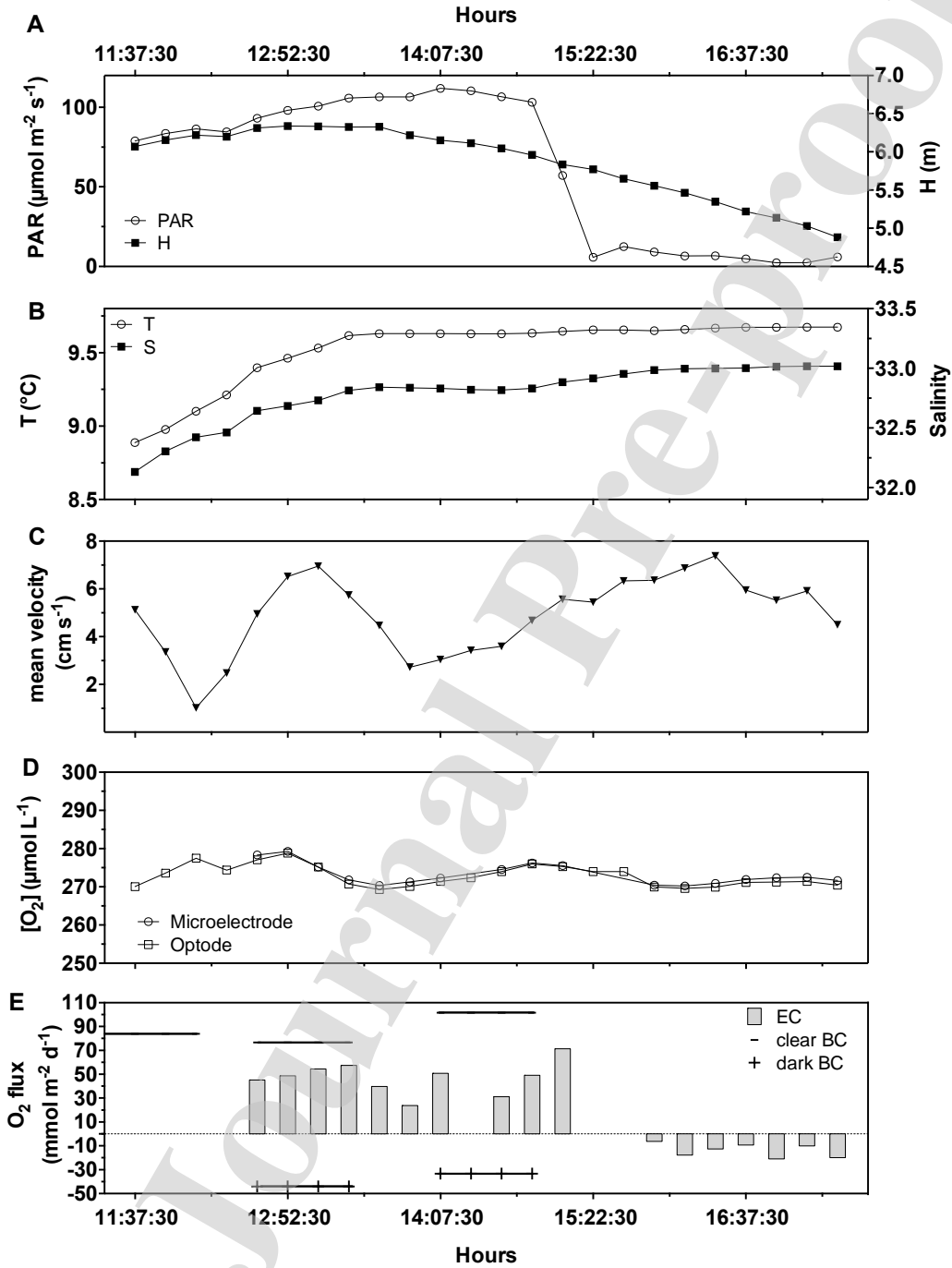
1059
11060
21061
31062
41063
51064
61065

Fig. 2



8
9
10
11
12
13
14
15
16
17
18
19
20
21
22
23
24
25
26
27
28
29
30
31
32
33
34
35
36
37
381066
391067
401068
411069
421070
431071
441072
451073
461074
471075
481076
491077
501078
511079
521080
531081
541082
551083
561084
571085
581086
61
62
63
64
65

Fig. 3

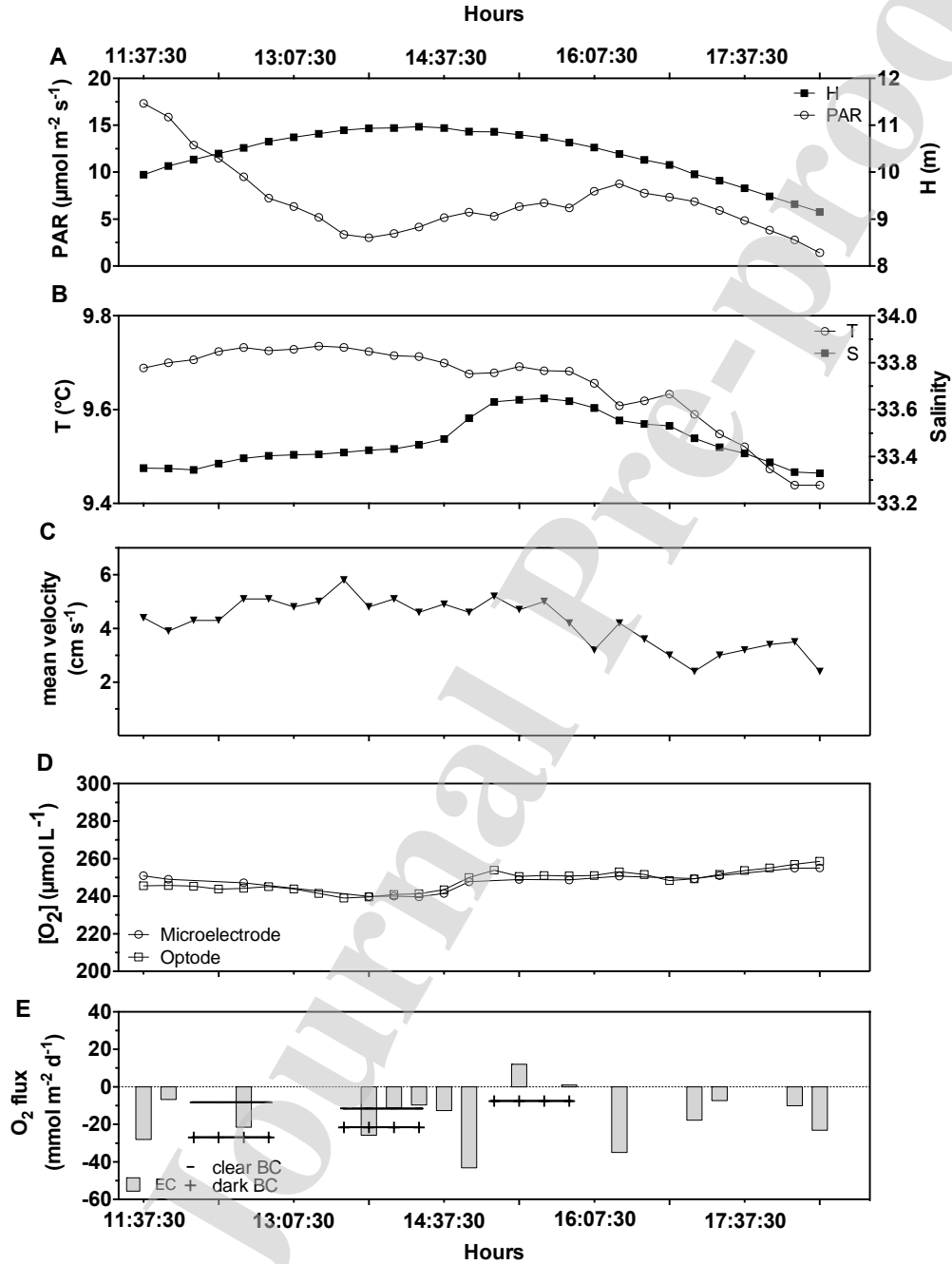


1087
11088
21089
31090
41091
51092
61093
71094
81095
91095

10
11
12
13
14
15
16
17
18
19
20
21
22
23
24
25
26
27
28
29
30
31
32
33
34
35
36
37
38
39
40
41
42
43
44
45
46
47
48
49
50
51
52
53
54
55
56
57
58
59
60
61
62
63
64
65

1096
1097
1098
1099

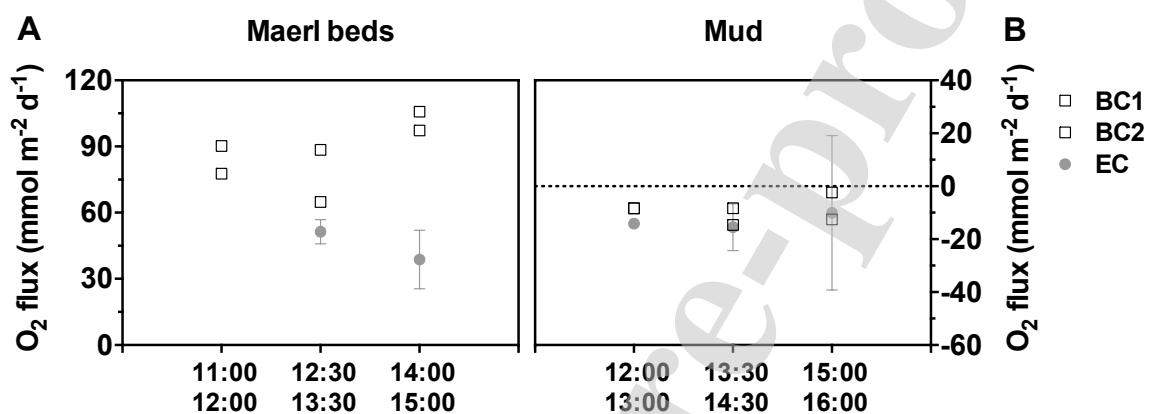
Fig. 4



1100
 11101
 21102
 31103
 41104
 51105
 61106
 71107
 81108
 91109
 101109

11
 12
 13
 14
 15
 16
 17
 18
 19
 20
 21
 22
 23
 24
 25
 26
 27
 28
 29
 30
 31
 32
 33
 34
 35
 36
 37
 38
 39
 40
 41
 42
 43
 44
 45
 46
 47
 48
 49
 50
 51
 52
 53
 54
 55
 561110
 571111
 581112
 591113
 60
 61
 62
 63
 64
 65

Fig. 5



1114
1115
21116
31117
41118
51119
61120
71121
81122
91123
101124
111124
121125
131126
141127
15
16
17
18
19
20
21
22
23
24
25
26
27
28
29
301128
311129
321130
331131
341132
351133
361134
371135
381136
391137
401138
411139
421140
431141
441142
451143
461144
471145
481146
491147
501148
511149
521150
531151
541152
551153
561154
571155
60
61
62
63
64
65

Fig. 6

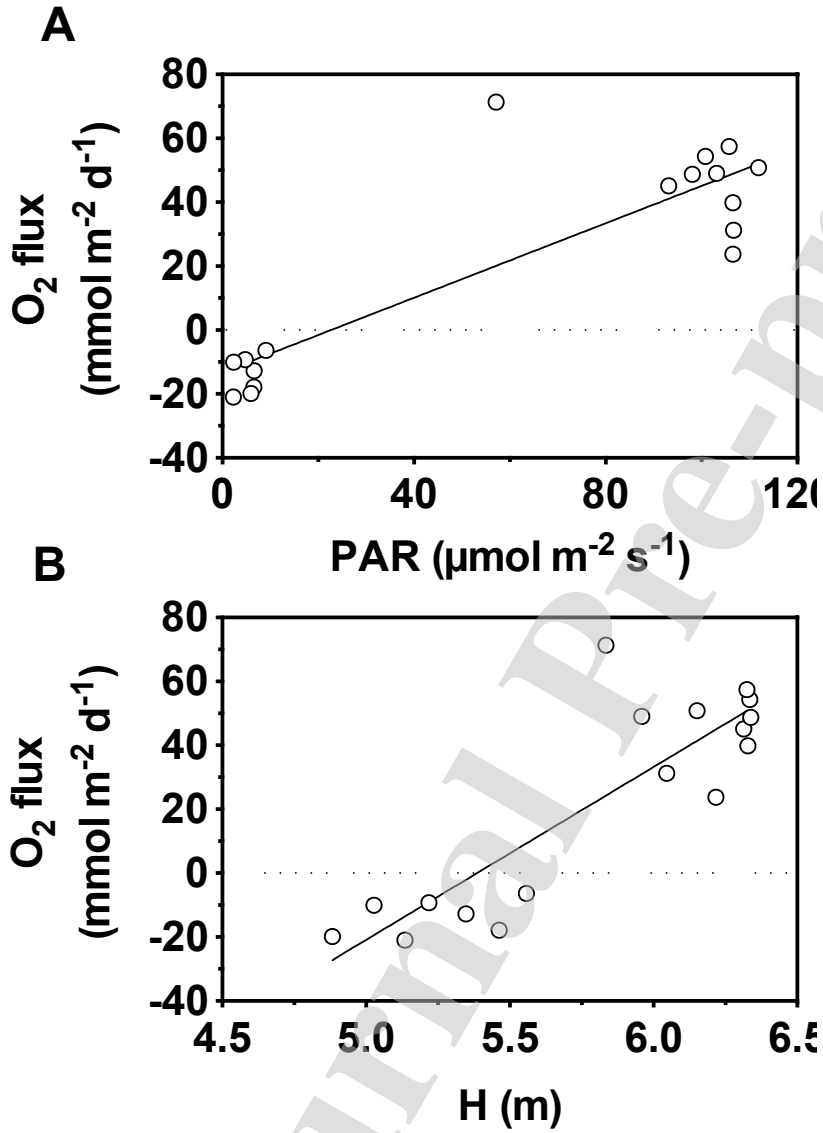


Table 1. Environmental parameters and benthic O₂ fluxes measured over Maerl beds (Ma) and bare muddy sediments (Mu) in the Bay of Brest (20-21/02/2013). Averages and ranges are presented in bold (\pm standard deviation) and in italic between brackets, respectively. PAR, photosynthetically active radiation. H, water height. T_w, water temperature. [O₂]_μ and [O₂]_{sdot} oxygen concentrations measured by the EC microelectrode and the SDOT optode, respectively. EC FO₂, benthic O₂ fluxes measured by EC during the whole deployments. BC FO₂, O₂ fluxes measured by clear and dark benthic chambers during daytime. EC raw data have been sampled at 64 Hz and environmental parameters have been measured every two minutes. All values were averaged over 15 min. bursts.

	Maerl bed (M _a)	Mud (M _u)
PAR ($\mu\text{mol m}^{-2} \text{s}^{-1}$)	62.1 \pm 44.0 (2.3 – 111.9) N=24	6.9 \pm 3.7 (1.4 – 17.3) N=28
H (m)	5.9 \pm 0.4 (4.9 – 6.3) N=24	10.4 \pm 0.5 (9.1 – 11.0) N=28
T_w (°C)	9.5 \pm 0.2 (8.9 – 9.7) N=24	9.6 \pm 0.1 (9.4 – 9.7) N=28
Salinity	32.7 \pm 0.3 (32.1 – 33.0) N=24	33.5 \pm 0.1 (33.3 – 33.7) N=28
Mean velocity (cm s^{-1})	4.9 \pm 1.6 (1.0 – 7.4) N=24	4.2 \pm 0.9 (2.4 – 5.8) N=28
[O₂]_μ ($\mu\text{mol L}^{-1}$)	273 \pm 3 (270 – 279) N=17	248 \pm 5 (240 – 255) N=15
[O₂]_{sdot} ($\mu\text{mol L}^{-1}$)	273 \pm 3 (269 – 279) N=24	249 \pm 6 (239 – 265) N=26
EC O₂ flux ($\text{mmol m}^{-2} \text{d}^{-1}$)	22.0 \pm 32.7 (-21.0 – 71.3) N=17	-15.9 \pm 14.0 (-43.1 – 12.1) N=15
Clear BC O₂ flux ($\text{mmol m}^{-2} \text{d}^{-1}$)	87.4 \pm 14.5 (64.8 – 105.7) N=6	-9.1 \pm 4.2 (-14.6 – -2.4) N=6
Dark BC O₂ flux ($\text{mmol m}^{-2} \text{d}^{-1}$)	-38.6 \pm 7.6 (-44.0 – -33.3) N=2	-18.7 \pm 10.0 (-27.0 – -7.6) N=3
Footprint length (m)	171 \pm 64 (63 – 257) N=12	115 \pm 35 (57 – 195) N=26
Footprint upstream distance (m)	7 \pm 3 (2 – 10) n=12	5 \pm 2 (2 – 10) n=26
Footprint width (m)	2.6	2.6

Table 2. Benthic O₂ flux regional comparisons across sites and methodologies (BC and EC techniques). Fluxes are in mmol m⁻² d⁻¹. EC fluxes measured in this study and presented in Table 2 correspond to daily rates estimated from daylight hours.

Benthic O ₂ fluxes (Maerl station)	Benthic O ₂ fluxes (Mud station)	Site characteristics	Methodology	References
35.0 ± 5.8 (NCP)	-3.7 ± 1.7 (CR)	Temperate (Bay of Brest)	Aquatic EC (Winter)	This study
87.4 ± 14.5 (NCP)	-9.1 ± 4.2 (NCP)		Clear BC (Winter)	
-38.6 ± 7.6 (CR)	-18.7 ± 10.0 (CR)		Dark BC (Winter)	
13.9 ± 7.2 (NCP)		Temperate (Loch Sween, Scotland)	Aquatic EC (Winter) Dark BC (Winter)	Attard et al. (2015)
-25.2 ± 9.1 (CR)				
79.2 ± 42.5 (NCP)		Temperate (Bay of Brest)	Clear BC (Winter)	Martin et al. (2007a, b)
-67.2 ± 12 (CR)	21.3 ± 5.3 (CR)		Dark BC (Winter)	
-108.6 ± 29.8 (NCP)		Temperate (Bay of Brest)	Clear BC (Spring)	Martin et al. (2005)
	-19.2 ± 2.4 (CR)	Temperate (Bay of Brest)	Dark BC (Winter)	Ni Longphuir et al. (2007)
	-39 ± 3; -46 ± 8 (CR)	Temperate (Aarhus Bay and Limfjorden Sound, Denmark)	Aquatic EC	Berg et al. (2003)

Highlights

- Benthic O₂ exchange was monitored in a temperate bay in winter
- The aquatic Eddy Covariance and benthic chambers were deployed over two stations
- Maerl beds and muddy sediments generally released and consumed O₂
- Techniques showed similar patterns of temporal O₂ flux changes at both sites
- Benthic chambers may have underestimated Maerl community respiration

Pierre Polsenaere: Conceptualization, Methodology, Software, Validation, Formal analysis, Investigation, Writing - Original Draft, Writing - Review & Editing

Bruno Deflandre: Conceptualization, Methodology, Investigation, Resources, Writing - Review & Editing, Supervision, Funding acquisition

G rard Thouzeau: Conceptualization, Methodology, Validation, Formal analysis, Investigation, Resources, Writing - Review & Editing, Funding acquisition

Sylvain Rigaud: Methodology, Writing - Review & Editing

Tom Cox: Software, Validation, Formal analysis

Erwan Amice: Methodology, Resources

Thierry Le Bec: Methodology, Resources

Isabelle Bihannic: Methodology, Resources

Olivier Maire: Conceptualization, Methodology, Validation, Formal analysis, Investigation, Resources, Writing - Review & Editing, Supervision, Project administration, Funding acquisition

Declaration of interests

The authors declare that they have no known competing financial interests or personal relationships that could have appeared to influence the work reported in this paper.

The authors declare the following financial interests/personal relationships which may be considered as potential competing interests:

Journal Pre-proof